Numb is a membrane-active clathrin adaptor

A thesis submitted in partial fulfilment of the requirements of the degree of

Doctor of Philosophy

by

Devika S. Andhare

20133251

Indian Institute of Science Education and Research Pune

2019

CERTIFICATE

Certified that the work incorporated in the thesis entitled "Numb is a membrane-active clathrin adaptor" submitted by Devika Andhare was carried out by the candidate, under my supervision. The work presented here or any part of it has not been included in any other thesis submitted previously for the award of any degree or diploma from any other University or institution.

Thomas Pucadyil

(Supervisor)

Date:14.05.2019

Declaration

I declare that this written submission represents my ideas in my own words and where others' ideas have been included; I have adequately cited and referenced the original sources. I also declare that I have adhered to all principles of academic honesty and integrity and have not misrepresented or fabricated or falsified any idea/data/fact/source in my submission. I understand that violation of the above will be cause for disciplinary action by the institute and can also evoke penal action from the sources which have thus not been properly cited or from whom proper permission has not been taken when needed.

(Signature)

Devika Andhare

Date:13/05/2019

Acknowledgement

I want to express my gratitude to my supervisor, Dr. Thomas Pucadyil for his constant encouragement and guidance throughout my graduate studies. His vast knowledge, expertise and critical feedback were integral to the completion of this work. Working with Thomas has helped me evolve better scientific abilities and more importantly effective science communication, writing and presentation skills. I will always be immensely grateful for the excellent training I received while working in the Pucadyil lab.

I am grateful to my research advisory committee members Dr. Jeet Kalia and Dr. Girish Ratnaparkhi for the many fruitful and encouraging discussions. Special thanks to Girish who was my sounding board and advisor through the many rough patches I hit during my graduate term. I am immensely grateful to Dr. Sashikant Acharya who has been my mentor and a pillar of strength throughout my journey since masters. I am also thankful to Dr. Raghav Rajan for some enjoyable discussions on his work and Dr. Deepa Subramanyam for her support and advice.

I thank my fellow lab members Sachin Holkar, Srishti Dar, Manish Singh Kushwah, Raunaq Deo, Sukrut Kamerkar, Krishnendu Roy, Soumya Bhattacharyya, Himani Khurana, Gregor Jose and Shilpa Gopan for the healthy discussions, critical feedback, and help in editing this thesis.

I thank all the wonderful friends who made my time at IISER Pune enjoyable and have helped me get through the rough times-Natasha Buwa, Kunalika Jain, Kriti Chaplot, Somya Madan, Tanushree Kundu, and Swati Sharma.

I have enjoyed collaborating and learning with Aarthy, Ashwini, Theja Sajeevan, Gokul VP, Pavithra Mahadevan, Somya Madan, and Rashim Malhotra.

I want to thank IISER Pune for their research facilities and excellent support staff. I want to thank UGC and HHMI foundation for research fellowship, DBT-CTEP and Infosys Foundation for the generous travel awards that enabled me to present my work internationally.

Special thanks to Sukrut Kamerkar, without whose support and guidance I could not have completed my Ph.D. He never let me lose hope and kept me going when things looked bleak.

Most importantly, I am grateful to my parents- Shyam and Meenal Andhare and sibling Aditi Sadhu for their constant faith and support that allowed me to pursue my ambitions.

Synopsis

The compartmentalized eukaryotic cells need an active exchange of macromolecules between intracellular organelles to maintain homeostasis. A major proportion of the macromolecular transport is achieved by vesicular traffic pathways in which contents from a donor organelle are packed into a membrane-bound carrier that transports them to a specific target organelle. Clathrin hexamers, composed of three heavy and three light chains, and its accessory-proteins form a molecular scaffold that organizes and sculpts the membrane-bound vesicles. Vesicles decorated with the clathrin-coat mediate transport from the plasma membrane, the *trans*-Golgi network, and the endosomes.

Clathrin, the major component of these coated-carriers, does not interact with membrane directly but is linked via a distinct set of adaptor proteins. Adaptors recognize specific classes of membrane proteins; recruit and assemble clathrin on the membrane and sculpt the planar plasma membrane into vesicles. High-resolution EM studies, fluorescent imaging of events near the plasma membrane using TIRF, and biochemical reconstitution have significantly clarified the process of formation of the clathrin-coated vesicle. Although the individual activities of endocytic-proteins are well studied, how these protein come together to orchestrate the process of vesicle formation is not completely understood. Also, the dynamics of clathrin polymerization and its concomitant effect on membrane remodeling remains unclear due to lack of temporal assays that follow adaptor mediated clathrin assembly in real time. Moreover, mechanism and proteins involved in building clathrin-coated carriers at intracellular organelles are still unclear.

Numb, an evolutionarily conserved cytosolic protein is essential for clathrin-mediated transport of a class of receptors containing the FXNPXY sorting signal; notably Notch and the cholesterol receptor NPC1L1. Numb is best studied in *Drosophila* development where it was first identified as a mutation that caused severe defects in the sensory nervous and muscular systems. Numb was later understood to work as an intrinsic cell-fate determinant by regulating Notch receptor signaling. Numb has been implicated in changing receptor distribution by participating in clathrin-mediated endocytosis through its interaction with AP-2. Surprisingly the Numb mutant unable to bind AP-2 still functions in cell-fate determination. Increasing experimental evidence also points to Numb's involvement in the endosomal sorting of receptors between the recycling and the degradative pathways.

However, what regulates Numb recruitment to different target organelles and the mechanism of how it links the cargo-receptors to the clathrin-transport machinery is still lacking.

Using a novel pull-down approach, this study aims to identify effectors of membrane-bound Numb. Further, in conjunction with information from the analysis of membrane-binding properties of Numb, this work attempts to reconstitute intrinsic functions of Numb.

Chapter 1 gives an introduction to various coated-vesicle transport pathways with a focus on clathrin-coated vesicles (CCV). The mechanism of CCV formation at the plasma membrane is described in detail along with the proteins involved in the process. Functions of cargo-specific adaptor proteins along with their general domain-architectures are introduced. Chapter 1 then focuses on the known roles of Numb, its biochemical properties and sub-cellular localization highlighting the lack of a mechanism for Numb function.

Chapter 2 describes the use of SUPER templates as a tool to investigate the interactors of membrane-bound proteins. SUPER templates consist of glass beads coated with lipid bilayer made up of zwitterionic lipids along with a trace of chelating lipids. This acts as a highly passive generic template to display any histidine-tagged bait protein of choice at controlled densities enabling pull-down of its interacting-proteins. As a proof of principle, the adaptor for ubiquitinylated receptors epsin1 is displayed on SUPER templates and its previously known interactions with endocytic proteins analyzed. Strikingly, display of adaptor proteins on membrane-surface is found to enhance its ability to bind endocytic proteins significantly.

Furthermore, this pull-down approach also reveals how competitive binding between monomeric adaptors (epsin1 and AP180), AP-2 (the central coordinator of CME), and clathrin could possibly regulate the hierarchy of events in the formation of a clathrin-coated vesicle.

Most importantly, pull-downs using SUPER templates uncover a previously unknown direct physical interaction between Numb and purified clathrin.

Chapter 3 attempts to narrow down the clathrin-binding site/s on Numb using a deletion-based approach. Screening of Numb deletions for the loss in clathrin-binding complemented with the screening of the purified fragments of Numb for their sufficiency to

bind clathrin identified residue 355-554 (also known as the PRR) to independently define the clathrin-binding site on Numb.

To better understand the significance of Numb-clathrin association in a cellular context, effect of Numb PRR overexpression on transferrin uptake was studied. TfnR is the canonical marker for clathrin-mediated transport. Overexpression of Numb PRR in Cos-7 cells was found to hamper transferrin uptake.

How the cytosolic Numb is transiently recruited to a specific target organelle is not yet understood. **Chapter 4** focuses on the biochemical determinants of Numb-membrane interaction. Using SMrTs as a membrane template that mimics distinct topological stages encountered during formation of a clathrin-coated vesicle, Numb is found to bind membranes containing anionic phospholipid PIP_2 or the cargo of Numb-NPC1L1. Mode of recruitment seemed to affect the organization of Numb with the protein showing curvature-dependent binding in the presence of PIP_2.

Interestingly, upon membrane-binding, Numb was found to spontaneously arrange in distinct scaffolds. Moreover, Numb scaffolds were membrane-active and were seen to constrict the underlying membrane tube. Comparison with other adaptors revealed the Numb PTB to mediate oligomerization and membrane-remodeling.

Chapter 5 describes the use of SMrTs to visualize the dynamics of Numb-mediated clathrin assembly using fluorescently labeled Numb and native clathrin. Numb scaffolds directed clathrin assembly to regions of tube constriction. Similar to other CLASPs, clathrin preferentially assembled in curvature-dependent manner. Analysis of real-time clathrin assembly revealed that the kinetics of clathrin-polymerization by Numb matched the previously reported rates with other monomeric adaptors.

Taken together, these results redefine Numb as a clathrin-interacting and membrane-remodeling adaptor protein. The contribution of Numb's ability to self-assemble, remodel membranes, and bind clathrin to its cellular function is however still unclear.

Table of Contents

Table of Figures

Chapter 1

Introduction

In eukaryotic cells, proteins and lipids are actively transported along the endocytic and the secretory pathways as well as between intracellular membrane-bound organelles. A large proportion of this transport activity is accomplished through mechanisms collectively referred to as 'membrane traffic,' a process in which part of the delimiting membrane and lumenal contents of a donor organelle are transferred to an acceptor organelle. The most-well studied carrier vesicles that travel on these traffic pathways are those that are clearly identifiable by their coats made of either clathrin and its accessory proteins or of coatamer-COPI and COPII (Fig 1.1). Clathrin triskelia, made up of identical 3 heavy chains (192kDa) and 3 light chains (22– 28kDa) has the property of self-assembly to form cage- or basket-like structures which form a lattice-like coat on and around membranes. The best-studied role of clathrin is in generating coated-vesicles at the plasma membrane along with the TGN and endosomes (Fig 1.1).

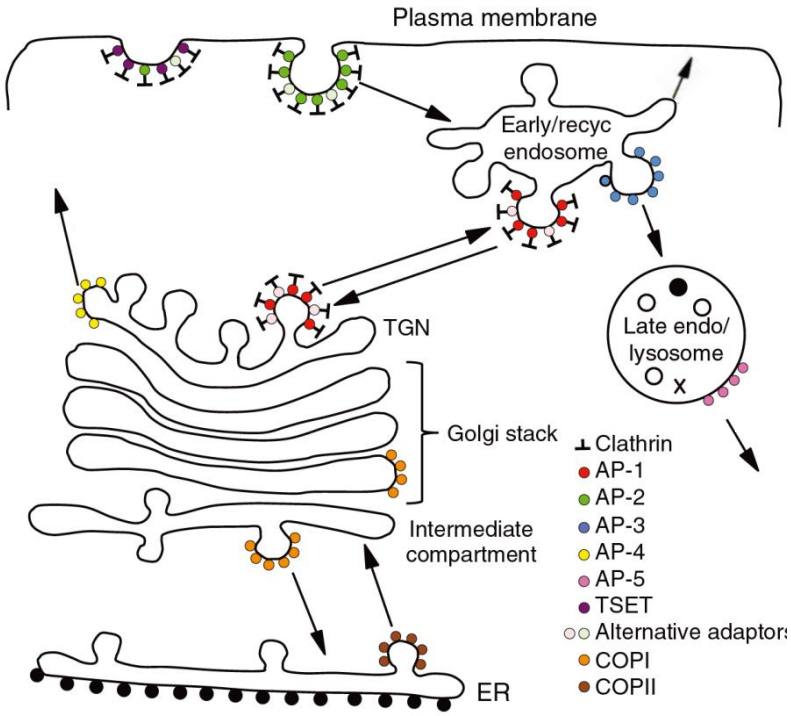

Fig 1.1 Cartoon representation of a few of the various coat components, including adaptors, at different cellular organelles (Adapted from Robinson 2004).

1.1 Mechanism of formation of clathrin-coated vesicles

EM-based studies along with fluorescence-based imaging of endocytic events near the cell surface have elucidated the mechanism of formation of CCV[1,2]. The initiation of a clathrin-coated vesicle occurs randomly when endocytic coat proteins from the cytosol start

to cluster on the inner leaflet of the plasma membrane. These proteins recruit and concentrate cargo molecules to the coated region of the plasma membrane. The cluster of endocytic proteins acts as a nucleation-point and marks the site of a nascent clathrin-coated pit which is then joined by accessory and regulatory components that further stabilize the pit. The assembling coat promotes membrane bending, an energetically unfavourable process, which transforms the flat plasma membrane into a curved 'clathrin-coated pit'. Actin polymerization also cooperates with the coat to promote membrane sculpting. The neck connecting the CCP to the donor membrane is then acted upon by scission proteins that constrict and cut the neck to release the clathrin-coated vesicle from the plasma membrane. Once released, a dedicated set of proteins (including Hsc 70 and auxilin) disassemble the endocytic coat releasing the cargo-filled vesicle to traffic along the cell (Fig 1.2 A)[3]. Although many of the proteins involved in CME have been characterized in detail and their individual activities documented, how these proteins cooperate in the cell to form the endocytic machinery that functions in a precise manner to package a wide variety of cargoes into vesicles and how this process responds to environmental cues to maintain cellular homeostasis is still unclear.

The rate of clathrin self-assembly is very slow under physiological conditions, and therefore additional factors called adaptor proteins are required to promote clathrin assembly in vivo. Adaptor proteins bind lipids, sort cargo by recognizing specific sorting motifs on receptors and induce clathrin polymerization around the membrane. Heterotetrameric AP-2 is the central adaptor that acts as a hub to initiate and co-ordinate CCV formation at the plasma membrane. AP-2 is the major component of purified clathrin-coated vesicles, second in abundance only to clathrin itself[4]. It has been shown to have binding sites not only for clathrin and cargo proteins but a battery of other endocytic adaptor and accessory proteins[5]. Other monomeric adaptors or CLASPs (Clathrin Associated Sorting Proteins) including Epsin, AP180/CALM, Hip1, Dab2, β-arrestin and ARH have all been shown to recognize specific receptors, bind PIP_2, clathrin and AP-2 (Fig 1.2B)[6–10]. The prevailing model for CME proposes that AP-2 initiates and co-ordinates CCP formation as well as polymerizes the clathrin-coat, while the monomeric CLASPs act as an extended linker to recruit various cargo receptors to the clathrin-coated pit. Contrary to this model however endocytosis of LDL and EGF receptors remain unaffected in AP-2 depleted cells suggesting AP-2 may not be imperative for formation of clathrin-coated vesicles, but that it is one of several endocytic adaptors required for the uptake of specific cargo receptors including the transferrin receptor[11,12].

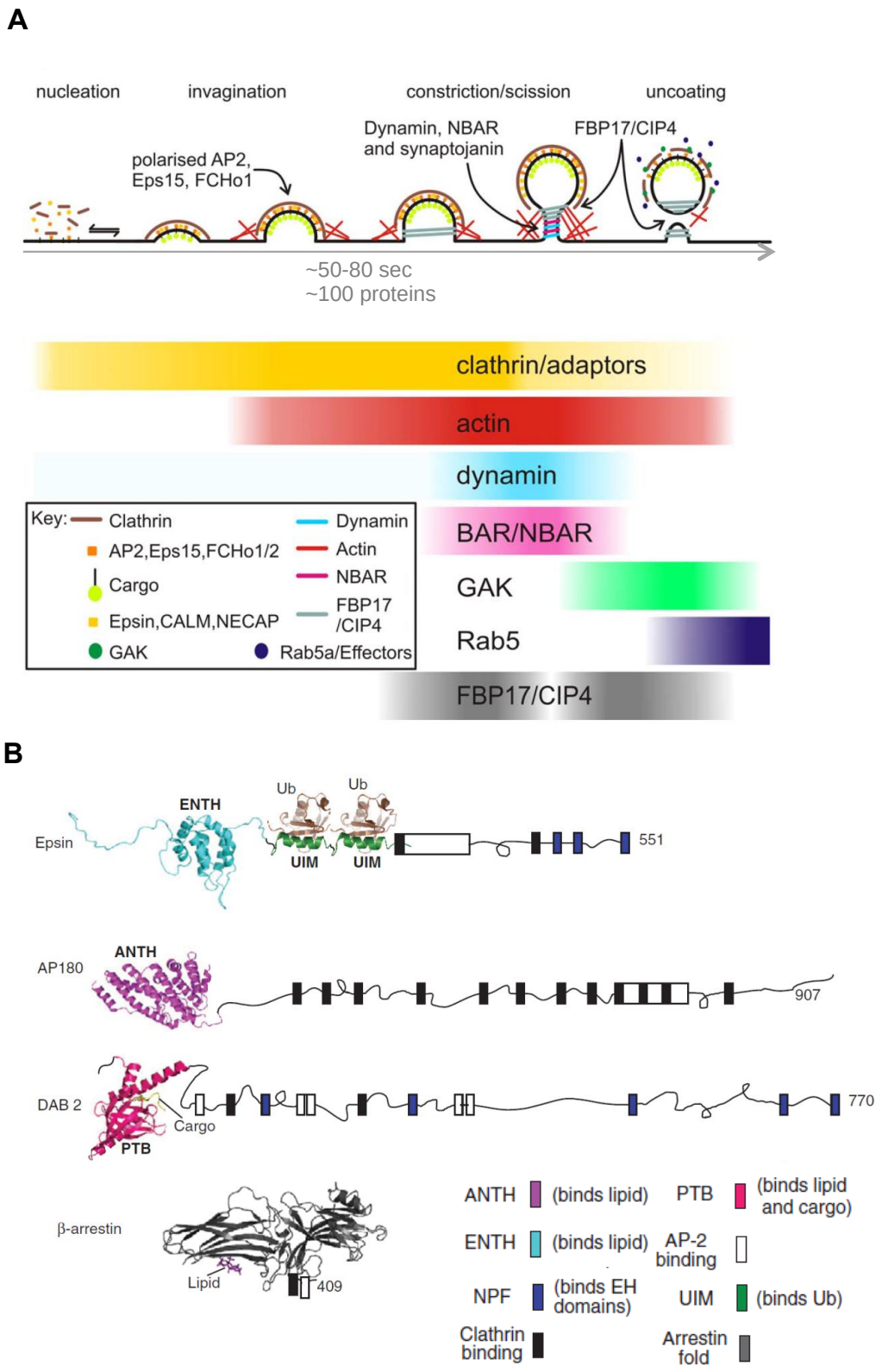

Fig 1.2 Canonical model of CME. (A) Schematic illustrating the stages of CCV formation along with relative temporal order of recruitment of different endocytic protein modules (Adapted from[1]) (B) Domain architecture of monomeric CLASPs (Epsin,AP180, Dab2 and β-arrestin) highlighting the structure of their membrane-

associating domains and the multiple endocytic protein binding motifs displayed on the unstructured C-terminus[13].

Unlike clathrin-coated vesicles that aid endocytosis at the plasma membrane, formation of clathrin-scaffolded carriers at the TGN and endosomes are less-understood. Adaptors involved in promoting clathrin-assembly at the intracellular organelles include AP-1, AP-3 and GGA [12,14,15]. Both TGN and endosomes serve as cellular sorting stations where vesicles containing distinct cargo diverge and travel retrograde to several target membranes[16,17]. Polarized sorting, essential to maintain different plasma membrane domains with distinct protein compositions that are a hallmark of epithelial and neuronal cells, is also mediated by cargo-sorting by adaptor proteins that work at recycling endosomes and/or the TGN[17].

One of the proteins involved in clathrin-mediated transport of cargo containing the FXNPXY sorting motif from the plasma membrane and polarized sorting at the endosomes is Numb.

1.2 Role of Numb in clathrin-mediated traffic

Numb facilitates clathrin-mediated trafficking of several transmembrane receptors including Notch, the cholesterol receptor NPC1L1, E-cadherin, β-integrin, amyloid precursor protein (APP), EAAT3 and ERBB[18–24]. Numb function is best-studied in *Drosophila* where it (dNumb) was initially discovered as a mutation that removed most of the sensory neurons in the developing peripheral nervous system[25]. Further studies revealed that Numb functions as an intrinsic cell fate determinant by asymmetrically partitioning during mitosis of neuronal precursor cells. In the Numb-enriched cell, Numb physically interacts with and antagonizes Notch receptor signalling thereby conferring alternative developmental fates on the resulting daughter cells[25,26]. Similar functions for mammalian Numb have been suggested since the ectopically expressed mammalian Numb is also asymmetrically segregated and rescues the Numb mutant phenotype in *Drosophila*. Numb acts as an almost dedicated adaptor that binds and causes clathrin-mediated internalization of the cholesterol receptor (NPC1L1) to facilitate cholesterol-uptake[19,27].

Although Numb is ubiquitously expressed it is found to be relatively enriched in lung and kidney tissues[28]. Alternative splicing gives rise to 4 isoforms of Numb, that vary in their PTB and the PRR domains[28] (Fig 1.3A), and are thought to have distinct functions[27,29]. The PTB domain at the N-terminus specifically recognizes membrane lipids and cargo receptors

while the C-terminus contains DPF (AP-2-associating) and NPF (Eps15 and EHD-binding) motifs (Fig 1.3B)[20]. Numb also contains a central proline rich region (PRR) that is similar to the proline rich domain (PRD) and is thought to associate with SH3-containing proteins[29]. Sub-cellular imaging indicates Numb is majorly cytosolic but gets dynamically localized to clathrin-coated structures at the plasma membrane as well as several organelles along the endocytic pathway[20,30].

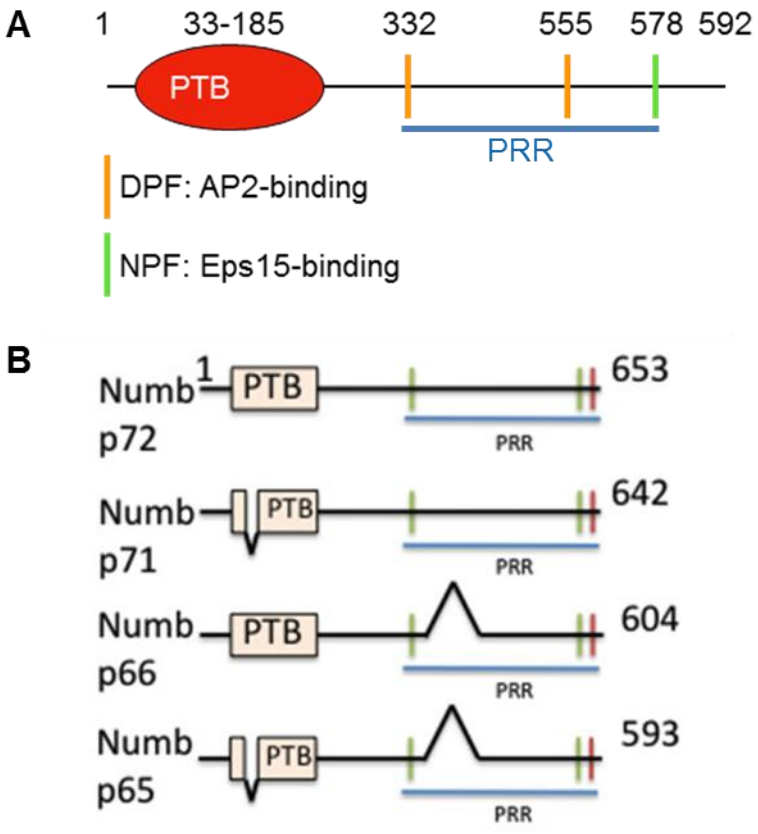

Fig 1.3 Domain organization of Numb (A) Representation of domain architecture of Numb (p65) (Schematic by Thomas Pucadyil) (B) Splice variants of Numb (Reproduced from [31])

While clear experimental evidence indicates that Numb induces endocytosis of NPC1L1, integrin and EAAT3 in a clathrin and AP-2-dependent manner depositing these at the early endosomes, the contribution of Numb to the regulation of Notch distribution is still unclear. Interestingly, imaging of fluorescently-tagged Numb in *Drosophila* revealed that Numb is dispensable for internalization of Notch but functions by co-accumulating with Notch (and Spdo) in sub-apical endosomes and inhibiting Notch recycling back to the plasma membrane [32]. Cellular studies tracking localisation of surface-labelled Notch indicates Numb promotes post-endocytic degradation of Notch[33,34]. Remarkably, the regulation of Notch distribution by Numb is independent of its ability to bind AP-2[35]. Studies from *C.elegans*

demonstrate that Numb inhibits receptor recycling by interfering with the lipid composition of the recycling endosomes[36]. A similar mechanism has also been proposed for Numb-mediated inhibition of ERBB signalling that is essential for proper proliferation of cardiomyocytes [21].

Together, based on the biochemistry and cellular localization studies, Numb can be proposed to influence the sub-cellular distribution of cargo receptors by two distinct mechanisms- 1) Promote clathrin-mediated endocytosis of receptors, 2) Inhibit recycling of receptors to the plasma membrane or aid in their degradation. However, the biochemistry, protein interactome, and the intrinsic properties of Numb that contribute to clathrin-mediated traffic and its participation in building a CCV are still unclear.

The work described here aims to better understand intrinsic functions of Numb by employing a pull-down based approach to identify interactors of membrane-displayed Numb in conjunction with a microscopy-based assay to recreate these interactions on membranes.

Chapter 2

A sensitive and versatile membrane template to analyze protein-protein interactions identifies Numb directly binds clathrin

2.1 Introduction

One approach to delineate the role of Numb in clathrin-coated vesicle formation is to characterize the interacting-partners of Numb. Protein-protein interactions are generally studied using pull-downs that are conventionally carried out with His- or GST-tagged bait proteins bound to sepharose beads that display Nitrilotriacetic acid (NTA) or glutathione (GSH) moieties, respectively. However, such matrices necessitate saturation with high bait density and tend to exhibit a high degree of non-specific binding. Also, the variation in surface densities of NTA and GSH moieties leads to uncontrolled concentration of bait proteins displayed on them. Importantly, these matrices do not allow pull-down of protein-protein interactions on a membrane surface. This is particularly relevant to endocytic protein interactions that are on their own weak but are stabilised when networked together on a membrane surface [37,38]. Liposome-floatation assays have been used to identify effectors of membrane-bound proteins [39]. However, these suffer from the inability to wash unbound proteins that leads to high background binding. Additionally, high-speed spins are required to separate protein-bound liposomes, which may interfere with the bound proteins.

To circumvent these issues and fish for effectors of membrane-bound Numb, a novel pull-down method consisting of lipid bilayer-coated silica beads (SUPER templates) is employed here.

Materials and methods

2.2.1 Cloning, protein expression, and purification

Rat epsin1 (O88339:Isoform 1), mouse Dab2 (UNIPROT ID P98078: Isoform p96), human ARH (UNIPROT ID Q5SW96) and mouse AP180 (UNIPROT ID Q61548: Isoform short), human Numb (UNIPROT ID P49757: Isoform 4) were cloned as N-terminal 6xHis and C-terminal StrepII-tag fusions. Residues 584-951 of the human AP-2β1 (UNIPROT ID P63010: Isoform 2) were cloned as N-terminal 6xHis-mEGFP and C-terminal StrepII tag fusions (Pucadyil and Holkar, 2016). GST-α adaptin-ear (residue 670-977) was a kind gift from Linton Traub. All clones were generated using PCR-based seamless cloning [40] and confirmed by sequencing. Proteins were expressed in BL21(DE3) in autoinduction medium (Formedium, UK) at 18°C for 30-36 h. Bacterial cells were pelleted and stored at -40°C. For purification, the frozen bacterial pellet was resuspended in buffer containing 20mM HEPES pH 7.4, 150mM NaCl (HBS), supplemented with protease inhibitor cocktail (Roche). After

resuspention, the cells were lysed by sonication in an ice water bath. Lysate was spun down at 18,500g for 30 mins and the supernatant was incubated with His-Pur^{TM} Cobalt resin (Thermo Scientific) for 1 hour at 4°C. The supernatant along with the resin was then poured in PD-10 column, and the resin was washed with 100 ml of HBS to get rid of non-specifically bound proteins. Protein was eluted using 20mM HEPES, 150mM NaCl, 250mM Imidazole pH7.4 containing buffer. Elution was applied to a 5 ml Streptactin column (GE Lifesciences), washed with HBS to get rid of non-specifically bound proteins. Protein was eluted using 20mM HEPES pH7.4, 150mM NaCl, 1mM DTT buffer containing 2.5mM desthiobiotin (Sigma). Purification using such tandem affinity ensures full-length and pure preparation of protein (Holkar et al., 2015). For long-term storage proteins were stored in 20mM HEPES pH7.4, 150mM NaCl supplemented with 10% glycerol, flash frozen in liquid nitrogen and stored at -80°C.

Clathrin heavy chain (Origene plasmid- SC125754) was cloned in pET15b with a C-terminal StrepII tag and expressed in BL21(DE3) using autoinduction medium (18°C, 36 hours). Bacterial cells were pelleted and resuspended in buffer containing 20mM HEPES pH 7.4, 150mM NaCl (HBS), supplemented with protease inhibitor cocktail (Roche). Cells were lysed by sonication in an ice water bath. Lysate was spun down at 18,500g for 30 mins. The supernatant was frozen with 10% glycerol. For use in SUPER template pull-down assays, the supernatant was freshly diluted by 50-fold (50 fold dilution was found to match the amount of clathrin detected in 1 mg/ml of brain cytosol).

2.2.2 SUPER (Supported Bilayer with Excess Reservoir) templates

SUPER templates were made as described previously[41]. Briefly, DOPC, DOPS (15mol%) and chelating lipid (DGSNTA(Ni^{2+})) (5 mol%) stocks were aliquoted in a clean glass tube, dried in vacuum and hydrated with de-ionzed water (Avanti Polar Lipids). To make small unilamellar vesicles (SUVs) hydrated lipids were sonicated with a probe sonicator at a low-amplitude setting in an ice-water bath. The samples were centrifuged at 100,000 g at room temperature and the supernatant containing SUVs was collected. 10 µl of silica beads (5.3 µm diameter; Corpuscular Inc.) were added to a premixed solution of SUVs (200µM) in 1M NaCl in a 1.5 ml clear polypropylene centrifuge tube. The reaction was incubated for 30 min at room temperature and mixed intermittently (by tapping). The templates thus formed were washed three times with 1 ml of de-ionized water by a low-speed spin (120 g, 2 min) in a

swinging bucket rotor at room temperature. 100 µl volume of solution was left behind after each wash to prevent drying of templates.

2.2.3 Pull-downs assays

Chelating lipid-containing SUPER templates were incubated with 1µM, 500 µl of purified bait proteins for 30 mins at RT. Templates were then washed (3*1ml HBS) by spinning at low-speed in a swinging-bucket rotor (120 g, 2 min). For pull-down of interacting partners, templates displaying bait protein were incubated with goat brain cytosol or bacterial (BL21DE3) lysate overexpressing CHC for 30 mins at RT. Templates were again washed (3*1ml HBS) to remove unbound proteins. 100 µl HBS was left behind after each wash to prevent templates from drying. The pellet after the last wash was re-suspended in 50 µl of 1x Laemmli's buffer, bolied at 99°C for 10 mins. The samples were resolved on 10% SDS-PAGE. Bound proteins were analyzed using immunoblotting.

For western blotting analysis, the gels were transferred onto PVDF. The membrane was incubated with blocking buffer (5% skimmed milk made in TBST) for 1 hour at room temperature. The membrane was then incubated with primary antibody diluted in the blocking buffer for 3 hours at RT. Subsequently the membrane was washed with TBST and incubated with suitable HRP-conjugated secondary antibody diluted in blocking buffer for 1 hour at RT. The blot was washed with TBST and developed with chemiluminescent substrate (WestPico, Thermo) and imaged in G:Box (Syngene).

2.2.4 Fluorescence imaging

mEGFP-coated resins were added to BSA-coated LabTek chambers (Thermo Fisher) and imaged using an Olympus IX71 inverted microscope through a 100X, 1.4 NA oil-immersion objective. Fluorescent probes were excited with an LED light source (Thorlabs), and fluorescence emission was collected through single-band pass filters (Semrock) with excitation/emission wavelength bandpasses of 482±35 nm/536 ± 40 nm for mEGFP on an Evolve 512 EMCCD camera (Photometrics). Image acquisition was managed by the MetaMorph soft-ware (Molecular Devices).

2.3 Results

2.3.1 Supported bilayers with Excess Reservoir: A passive template to pull-down interactors of membrane-bound proteins

In order to map effectors of membrane-displayed Numb, SUPER (Supported bilayer with Excess Reservoir) is used as the membrane template. SUPER templates are silica beads coated with a lipid bilayer containing an excess reservoir formed by high ionic strength aided fusion of liposomes onto the negatively charged bead surface (Fig 2.1 A) [42]. These silica-bead containing templates can be readily sedimented by low-speed spin allowing washing to remove unbound proteins during a pull-down. Here SUPER templates are adapted for use as a pull-down matrix by the inclusion of small amounts of chelating lipid (CL, Fig 2.1 B) that allows display of any desired histidine-tagged bait protein (Fig 2.1 B). Protein-coated templates form the bait to pull-down interactors from tissue extract (Fig 2.1 C). SUPER templates thus made showed negligible background binding when bare templates were incubated with brain cytosol (data not shown) emphasizing their passivity.

SUPER templates were made as described previously [41]. Briefly, the following steps were followed to prepare SUPER templates:

- DOPC, DOPS (15mol%) and chelating lipid (DGSNTA(Ni2+)) (5 mol%) stocks were aliquoted in a clean glass tube, dried in vacuum and hydrated with de-ionzed water (Avanti Polar Lipids)
- The hydrated lipids were sonicated with a probe sonicator at a low-amplitude setting in an ice-water bath in order to make small unilamellar vesicles (SUVs). The samples were centrifuged at 100,000 g at room temperature and the supernatant containing SUVs was collected
- 10 µl of silica beads (5.3 µm diameter; Corpuscular Inc.) were added to a premixed solution of SUVs (200µM) in 1M NaCl in a 1.5 ml clear polypropylene centrifuge tube
- The reaction was incubated for 30 min at room temperature and mixed intermittently (by tapping)
- The templates thus formed were washed three times with 1 ml of de-ionized water by a low-speed spin (120 g, 2 min) in a swinging bucket rotor at room temperature
- 100 µl volume of solution was left behind after each wash to prevent drying of templates

Stability of these modified SUPER templates against protein-induced perturbation was tested using a sedimentation assay[42]. Briefly, an aliquot of templates containing trace amount (1

mol%) of fluorescent lipid analog RhPE was gently added to tubes containing increasing amount of brain cytosol. In a separate reaction, the total lipid concentration on the templates was estimated by measuring the fluorescence released by adding templates to buffer containing 0.1% Triton X-100. The reactions were incubated for 20 min at room temperature and subjected to a low-speed spin. Membrane released in presence of cytosol was analysed by measuring the RhPE fluorescence in the supernatent (normalized to total lipid fluorescence). Interestingly, inclusion of CL drastically reduced membrane-release in sedimentation assay (as compared to templates made of only DOPC) (Fig 2.1 D red trace), indicating the templates to be stable matrices suitable for pull-down of interacting proteins.

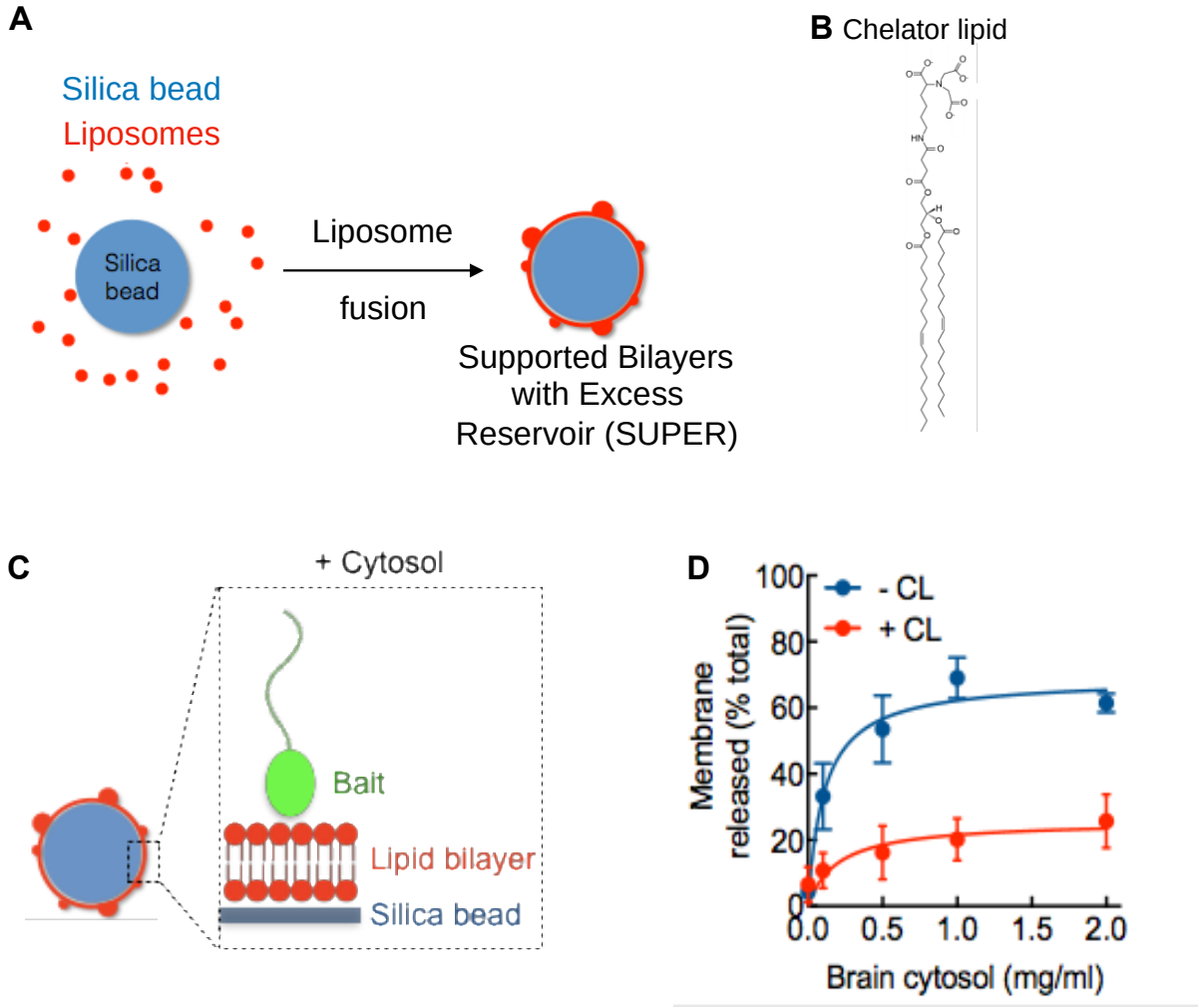

Figure 2.1 Chelator lipid-containing SUPER templates. (A) Schematic showing formation of SUPER (Suppoted bilayers with excess reservoir) by high ionic strength aided fusion of liposomes onto the silica bead. (B) Structure of the commercially available chelator lipid (DGSNTA(Ni^{2+}), Avanti). SUPERs formed with liposomes containing CL allow display of any desired His-tagged bait protein. (C) Bait-coated SUPER templates incubated with cytosol to pull-down potential interactors (D) SUPERs formed with CL are stable in

the presence of cytosol indicating that they could act as suitable matrices for the pull down of interacting proteins. Total represents membrane released upon solublization with 0.1% Triton X-100. Data for (D) from Apoorva Bhapkar. Schematics prepared by Thomas Pucadyil.

2.3.2 Validation of SUPER template-based pull-down by epsin1-clathrin interaction

Epsin is a monomeric adaptor protein that manages trafficking of ubiquitinylated cargo and is essential for clathrin-mediated endocytosis [43]. Epsin1 has a structured N-terminal ENTH domain that recognizes cargo and PIP_2, and an unstructured C-terminal tail that brings together endocytic proteins including AP-2, Eps15 and clathrin (Fig 2.2A). Epsin1-clathrin interaction is well studied and is mediated by two separate sites present on the unstructured C-terminal tail-1) a membrane proximal (CBS1: 257LMDLAD) and 2) a distal (CBS2: 480LVDLD) site (Fig 2.2A)[44,45]. In order to validate the use of SUPER templates as a pull-down matrix epsin1 displayed on SUPER templates was tested for its ability to bring down clathrin specifically from a complex mixture of cytosolic proteins. Purified epsin1, its CBS mutants (ΔCBS1, ΔCBS2, and ΔCBS null) and GFP (negative control) served as bait proteins (See methods section 2.2.1 for details on purification). Equal amounts of these Histidine-tagged bait proteins were added to SUPER templates following which templates were washed to remove excess unbound bait and incubated with brain cytosol. Templates were washed, resuspended in Laemmli's buffer, and resolved on an 8 % SDS-PAGE. Bound clathrin was blotted using an antibody against clathrin heavy chain. As compared to wild-type epsin1, CBS mutants show almost negligible binding to clathrin (Fig 2.2B). Purified Histidine-tagged GFP when used as dummy bait also shows no interaction with clathrin (Fig 2.2C). Apart from the prominent 180 kDa clathrin band, epsin1 also specifically pulled-down AP-2 (confirmed using an antibody against the AP-2 α subunit). Together these results establish SUPER template-based pull-down as a method to analyse protein-protein interactions. Of note, the coomassie gel for SUPER template pull-downs showed a prominent non-specific 50kDa band. Mass spectrometric analysis revealed tubulin to be the most abundant protein in this band which was further confirmed using immunoblotting (with an anti β-tubulin antibody, DSHB clone E7) (data not shown).

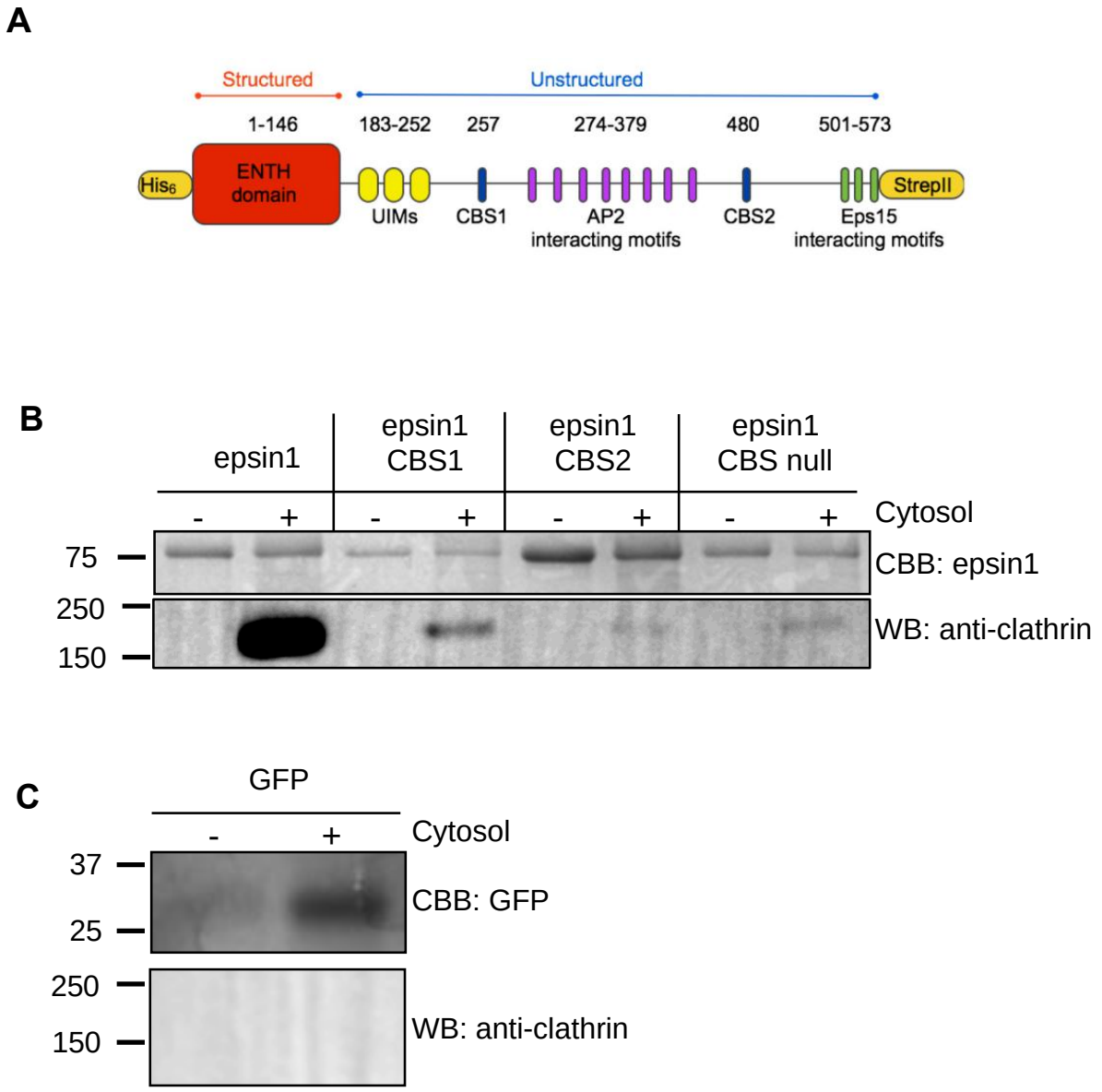

Fig 2.2 Analyzing adaptor-clathrin interactions. (A) Schematic showing epsin1 domain architecture. UIM-ubiquitin interacting motifs, CBS-clathrin binding sites (Adapted from [45]) (B) epsin1 shows efficient pull down of clathrin, a known binding partner. Interaction is direct since clathrin-binding site (CBS) mutants of epsin show reduced interaction with clathrin (data from Rashim Malhotra). (C) Dummy bait GFP used as a negative control shows no interaction with clathrin. (Anti clathrin antibody-Ab 24578)

2.3.3 Membrane-bound epsin1 on SUPER templates is more efficient in clathrin pull-down

In order to compare SUPER template-based pull-down assays to conventional methods, epsin1 was displayed on HisPur™ Cobalt resin and analysed for its ability to bind clathrin from brain cytosol. The difference in density of bait-binding sites between the two matrices was first estimated by saturating them with histidine-tagged mEGFP (Fig 2.3 A). Ratio of

fluorescence intensity to bead area shows that SUPER templates have 50-fold lower binding to GFP (Fig 2.3B). Despite this difference, when equal amount of epsin1 was displayed on the two matrices, SUPER templates showed dramatically higher clathrin binding (Fig 2.3C) (Note-Volume of saturated Cobalt resin was adjusted to match the amount of epsin1 displayed on SUPER templates). A possible explanation for this difference could be inaccessibility of the clathrin-binding sites on the epsin1 C-terminal tail when displayed at a very high density on a saturated HisPur^{TM} Cobalt resin surface. To test this SUPER templates were modified by using liposomes of increasing chelating lipid (DGSNTA(Ni^{2+})) concentration, leading to a concomitant increase in the bait density as seen by the rising GFP fluorescence/bead area ratio (Fig 2.3 D). There was however, no change in clathrin binding indicating that the inefficiency of epsin1 displayed on HisPur^{TM} in clathrin recruitment is unlikely due to inaccessibility of clathrin-binding sites (Fig 2.3 D).

Apart from clathrin, epsin1 also specifically associated with AP-2 in SUPER-template pull-down assays. AP-2 is known to bind eight separate sites on epsin1 [46]. Surprisingly, on comparing AP-2-epsin1 association when epsin1 was displayed on either HisPur^{TM} Cobalt resin or SUPER templates, it was seen that epsin1 displayed on SUPER templates was more efficient in AP-2 pull-down (Fig 2.3 E).

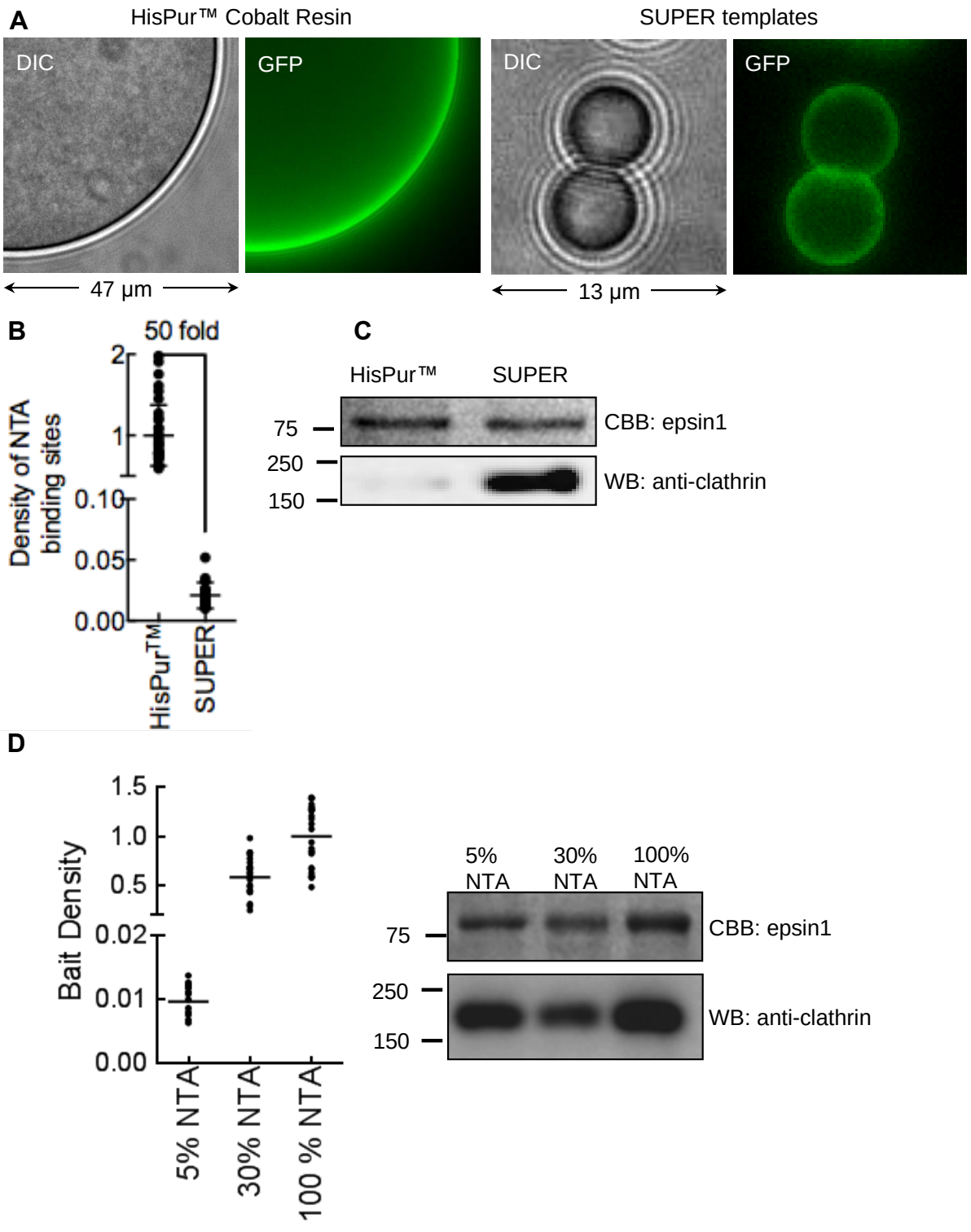
A
HisPur™ Cobalt Resin
SUPER templates
DIC
GFP
DIC
GFP
47 µm
13 µm
B
50 fold
Density of NTA binding sites
2
1
0.10
0.05
0.00
HisPur™
SUPER
C
HisPur™
SUPER
75
250
150
CBB: epsin1
WB: anti-clathrin
D
Bait Density
1.5
1.0
0.5
0.02
0.01
0.00
5% NTA
30% NTA
100 % NTA
5% NTA
30% NTA
100% NTA
75
250
150
CBB: epsin1
WB: anti-clathrin

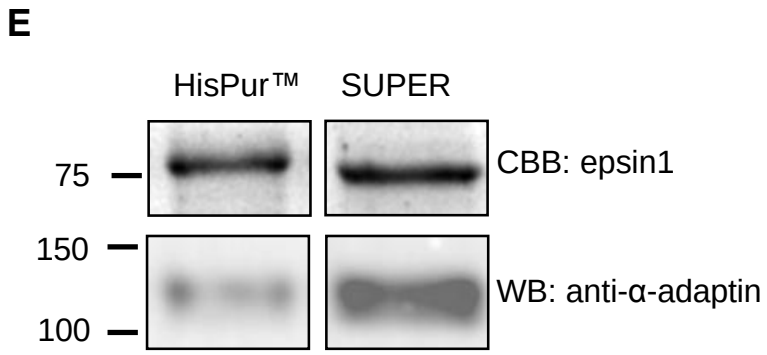

Fig 2.3 SUPER templates outperform conventional resins in pull-down experiments. (A) HisPur™ Cobalt resin and SUPER templates containing CL saturated with His-tagged GFP. (B) SUPER templates display 50-fold lower binding to His-GFP than HisPur™ but show more pull-down of clathrin than HisPur™ (C). (D) Increasing the epsin1 density on SUPER does not affect clathrin pull-down. (E) Epsin1 displayed on SUPER templates, as compared to HisPur™, also shows better binding to AP-2. Data (A) and analysis (B) by Thomas Pucadyil.

2.3.4 SUPER template pull-down reveals adaptors exist as separate complexes with clathrin and AP-2

Clathrin adaptors often harbour binding motifs for multiple partners on their unstructured C-terminal tail (Fig 1.2B) making simultaneous existence of these interactions unlikely. However, such an arrangement could impart directionality to a maturing clathrin-coated vesicle based on the affinities and local concentrations of the interacting partners. Epsin1 has eight AP-2 and two clathrin binding sites adjacent to each other [44,46]. To test how AP-2 influences the epsin1-clathrin complex, binding assays were carried out with purified, full-length epsin1 displayed on SUPER templates and brain extract containing extrinsically added, purified AP-2 α-appendage (AP-2-α). Indeed increasing recruitment of AP-2-α (Fig 2.4A) caused a concomitant inhibition in clathrin binding (Fig 2.4B). Curiously, AP180 (that harbours two α-appendage and eight clathrin binding sites) showed a loss in clathrin binding in presence of much higher concentration of the α-appendage (Fig 2.4E). Notably, it was also seen that extrinsically added α-appendage displaces the bound endogenous AP-2 from these adaptors (Fig 2.4C, F). Together these results reveal the competitive association of clathrin and AP2 with adaptor C-terminal tails.

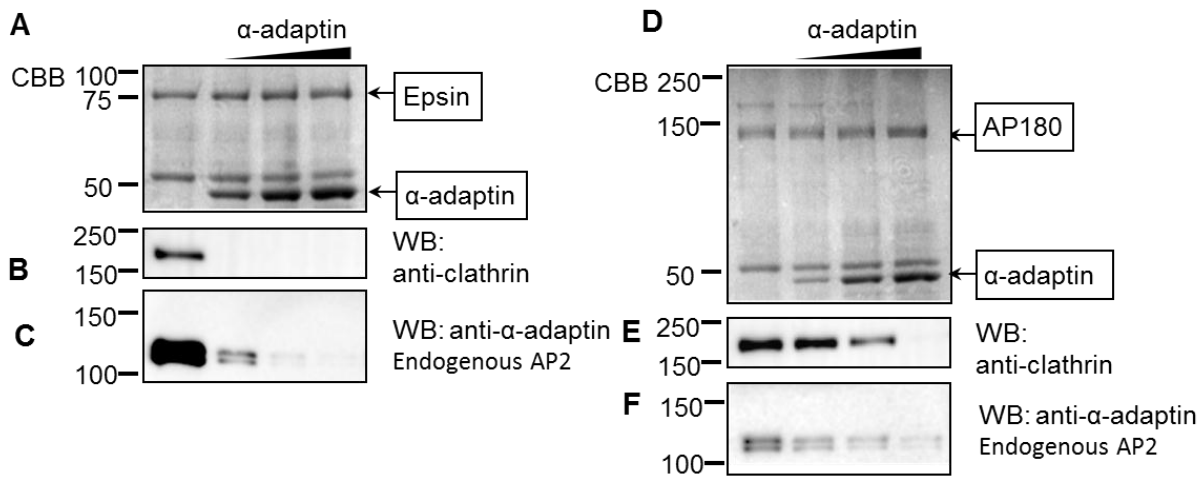

Fig 2.4 Competition assays reveal the nature of clathrin-adaptor interactions. Binding of epsin1 (A, B, C) and AP180 (D, E, F) to the α-adaptin domain of the heterotetrameric adaptor AP-2 and the concomitant inhibition in clathrin binding indicating that epsin1 and AP180 exist as mutually exclusive complexes with clathrin and AP-2. (Anti AP-2 α antibody-BD Bioscience 610502).

2.3.5 SUPER template pull-down uncovers direct interaction between Numb and clathrin

To delineate the role of Numb in clathrin-coated vesicle formation, SUPER template-based pull-down was used to detect a possible interaction between purified full-length Numb and clathrin heavy chain (CHC was recombinantly-expressed in BL21DE3 and prepared as described in Methods 2.2.1). Remarkably, SUPER templates displaying Numb showed direct binding with clathrin heavy chain. Purified GFP and the known clathrin-interactor AP-2-β (ear+appendage domain)[47] were used as controls (Fig 2.5A). Surprisingly SUPER templates displaying Numb upon incubation with brain cytosol showed negligible interaction with clathrin (Fig 2.5B). In contrast, other PTB-family adaptors (ARH, Dab2) could pull-down recombinantly-expressed clathrin heavy chain as well as native clathrin from brain cytosol (Fig 2.5C) [8,9]. Of note, Numb also specifically bound purified, native clathrin from bovine brain tissue (described in Fig 4.1). These results could point to a potential cellular-regulation of the Numb-clathrin interaction.

Pull-downs from brain cytosol detected a very strong association of Numb with AP-2, the central regulator of CME, as reported previously[20] (Fig 2.5D). Experiments with AP180 and epsin1 suggest competitive binding of AP2 and clathrin to these adaptors (Fig 2.4). To test if AP-2 similarly regulates Numb-clathrin interaction, SUPER templates displaying Numb were incubated with a mixture of clathrin heavy chain and AP-2-α. Indeed binding of

AP-2-α completely inhibited Numb's association with clathrin in a dose-dependent manner (Fig 2.5E).

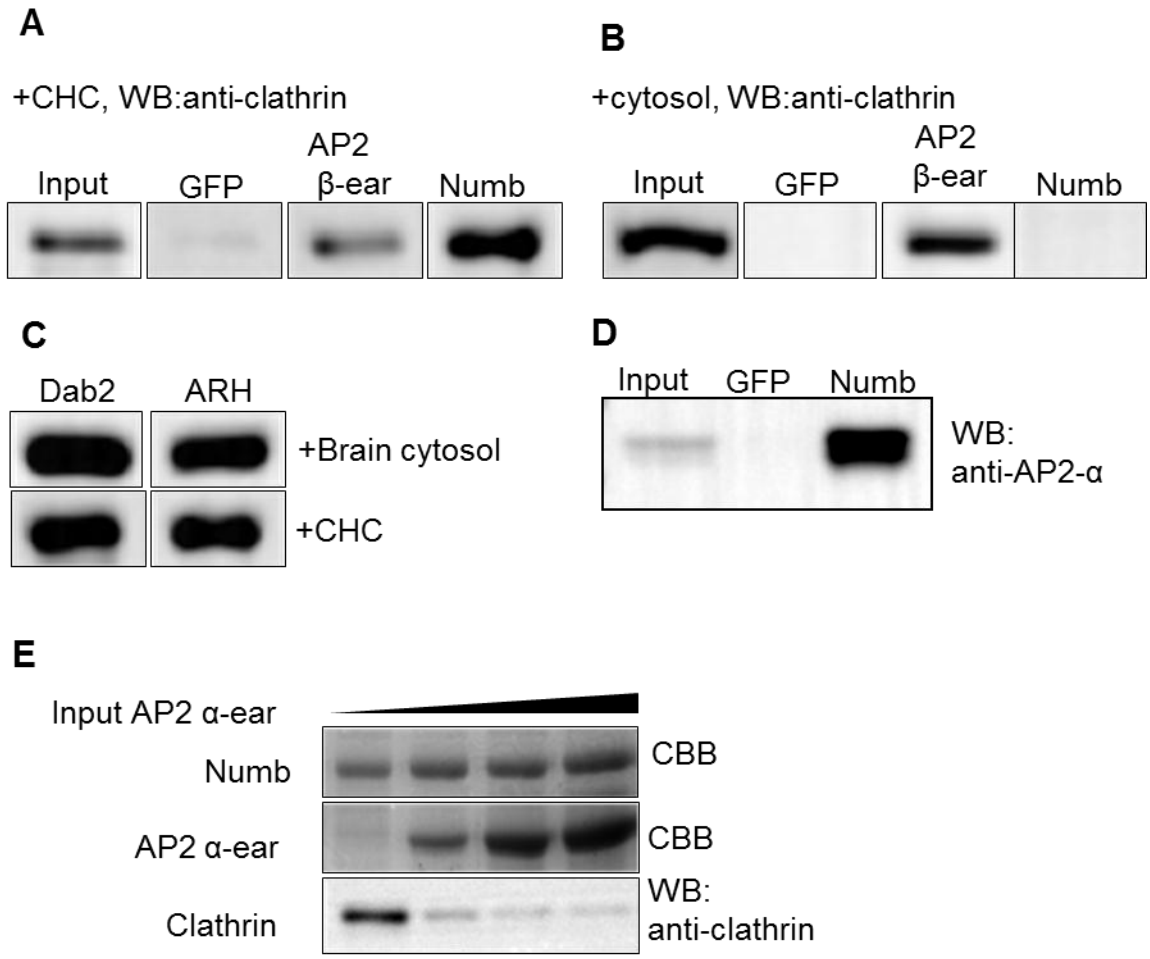

Fig 2.5 Numb interacts directly with clathrin. SUPER templates displaying bait proteins were incubated with recombinantly expressed clathrin heavy chain (1/50 fold dilution) or brain cytosol (1mg/ml). Bound proteins were analysed using immunoblotting. (A) Western blot showing direct binding of Numb to clathrin heavy chain. GFP shows negligible binding to clathrin while AP-2-β, the known clathrin-interactor serves as positive control. (B) Numb-clathrin binding is inhibited in brain cytosol; unlike the other PTB-family adaptors Dab2 and ARH (C). (D) Numb strongly associates with AP-2 from brain cytosol (E) Association of Numb to the α-adaptin domain of AP-2 causes inhibition in clathrin binding

2.3.6 Discussion

SUPER templates have been described earlier as a tool to analyse membrane budding and fission reactions which are facilitated by presence of the membrane reservoir[41]. Here SUPER templates are presented as a passive, sensitive and versatile matrix that allows analysis of protein-protein interactions of any membrane-localized bait. As compared to traditional resins, the amount of bait protein required in a SUPER template-pull-down is

drastically lower. Comparative analysis of clathrin pull-down abilities of epsin1 displayed on SUPER templates and HisPur^{TM} Cobalt resin reveal SUPER templates to be a more efficient pull-down-matrix for adaptor-clathrin interactions. Experimental evidence suggests that ease of membrane budding, driven by membrane tension, determines the likelihood of clathrin polymerization where high membrane-tension completely inhibits polymerization[48]. Reconstitution of clathrin assembly on membranes with purified adaptor proteins shows that a pre-curved membrane greatly facilitates clathrin-polymerization[10]. It is tempting to speculate that the differences in the amount of clathrin pulled-down by epsin1 displayed on HisPur^{TM} Cobalt resin and SUPER templates could be a reflection of clathrin polymerizing into pit-like structures, and not just binding, by adaptors displayed on the SUPER template membrane surface.

Pull-downs with purified adaptors (epsin1 and AP180), α-appendage and recombinantly expressed clathrin reveal how association with AP-2 could inhibit adaptor-clathrin binding. Like epsin1 and AP180, other monomeric clathrin-adaptors generally harbour multiple short, linear motifs on their unstructured C-terminal tail that recruit endocytic proteins (See Fig 1.2B). Similarly, the heterotetrameric adaptor AP-2, that functions to orchestrate molecular interactions in CME, can bind numerous accessory proteins via the two sites present on the α and β-appendage domains [5,49]. Such closely placed binding sites, that are often found to be overlapping, would sterically hinder simultaneous existence of these interactions. Although not tested with purified full-length proteins, indirect evidence for such a model comes from pull-downs with β-arrestin, an adaptor for internalization of GPCRs, where a mutant that is unable to bind AP-2 results in better clathrin pull-down. Similarly, association of β -appendage with clathrin leads to a reduction in the binding of endocytic accessory proteins (including AP180, amphiphysin, β-arrestin)[5]. Such competitive binding of accessory proteins driven by relative affinities is thought to ensure the directionality of a maturing clathrin-coated pit. It has been suggested that adaptor proteins may swap from an AP-2 appendage centric-hub to a clathrin centric-hub as the coated-pit matures[5,50].

Pull-downs using SUPER templates uncovered a direct interaction between Numb and clathrin heavy chain. Of note, the amino-acid sequence of Numb contains none of the canonical clathrin-binding motifs[51]. Pull-downs with purified Numb, α-appendage and recombinantly expressed clathrin also reveal that AP-2 association inhibits Numb-clathrin interaction. Moreover, the interaction between clathrin and Numb is supressed in brain cytosol. Of note, Numb also specifically bound purified, native clathrin from bovine brain

tissue (discussed in Fig 4.1). In contrast, other PTB-domain containing adaptors interact with both purified clathrin heavy chain as well as clathrin present in brain cytosol. One potential explanation is that additional binding partners may inhibit Numb-clathrin association either by steric hindrance or by affecting a conformational change in Numb. Among proteins involved in clathrin-mediated endocytosis, AP-2 and Eps15 are the known Numb-interactors. While association with AP-2 is necessary for Numb to traffic receptors such as EAAT-3 and NPC1L1[19,23], a mutant of Numb unable to bind AP-2 is functionally active in cell-fate determination[35]. Recently phosphorylation of Numb has been reported to dynamically regulate the Numb-AP-2 interaction as well as localization of Numb [18,52]. Phosphorylation of Numb by AAK1 dramatically changes its localization from plasma membrane to perinuclear endosomes[53]. Such regulations on the localization of Numb could also potentially affect its binding to clathrin in cells.

Chapter 3

Identifying the clathrin-binding determinants on Numb

3.1 Introduction

Fine mapping of the clathrin-binding sites from a number of adaptor proteins has helped define the clathrin-binding motif (CBM) to be a short linear arrangement of amino acids that fit to the consensus motif pLΦpΦp where L is leucine, Φ denotes a bulky hydrophobic residue, p denotes a polar residue. Although identification of such motifs has helped delineate clathrin-assembling activity in proteins involved in vesicular traffic (for e.g. GGA proteins), the predictive power of this consensus sequence is limited. A number of variants to the CBM have now been identified in various clathrin adaptors, including the PWDLW sequence in mammalian amphyphysin[54]. Furthermore, motifs that conform to the CBM do not always represent a function clathrin-binding site[55]. For example, crystallographic analysis of AP180 shows that the canonical CBMs lie buried deep within a highly ordered structure and are unlikely to be accessible for interaction with clathrin[56]. Instead, AP180 was found to contain multiple copies of DLL, a more degenerate version of the canonical CBM, on the unstructured C-terminal tail. However, deletions of DLL motifs had little effect on clathrin binding. Later studies revealed the LDSSLA[S/N]LVGNLGI sequence to be the major clathrin interaction site in AP180 and CALM. Strikingly, the minimum clathrin binding region on ARH is defined by the stretch between amino acids 180 to 308 [8]. Similarly, the C-terminal tail of synaptojanin, a polyphosphoinositide phosphatase, binds clathrin directly despite the absence of the consensus CBMs [57].

To identify the clathrin binding attributes on Numb a series of deletions spanning the entire length of Numb were generated and systematically screened.

3.2 Methods

3.2.1 Cloning, expression and purification

Sequential deletion constructs of Numb (isoform 4, Uniprot ID:P49757) cloned with 6xHis and StrepII tags at the N and C terminii, respectively (Fig 3.1A) were generated. Numb fragments (residues 448-473, 545-594, 346-575 and 335-554) that represent potential clathrin-binding stretches were cloned downstream of GFP with 6xHis and StrepII tags at the N and C terminii, respectively. GFP-Numb335-554 was cloned in pcDNA3 for expression in mammalian cells. GST-clathrin terminal domain was a kind gift from Linton Traub. All constructs were generated by PCR-based cloning and confirmed by sequencing. All proteins

with N-terminal His-tag and C-terminal StrepII tag were purified as described in Methods 2.2.1. GST-clathrin terminal domain (GST-CTD) was expressed and the supernatant prepared as described in Methods 2.2.1. The supernatant was bound to Glutathione Sepharose 4B resin (Thermo), washed and eluted in 50 mM Tris, 15 mM Glutathione, pH 8.0. The purified GST-CTD was dialyzed against HKS and flash frozen with 10% glycerol.

3.2.2 Dot-blot assay

Aliquots (200 µl) of purified proteins (1µM) were spotted on a nitrocellulose membranes using a 96 well dot-blot array system (Whatman) according to manufacturer's instructions. The membrane was then blocked with 5% skim milk in assay buffer (HKS + 0.1% Tween) for 1 hour at RT and incubated with 1 µM GST-CTD prepared in assay buffer for 1 hour at RT. Subsequently, the membrane was washed 3 times with assay buffer and incubated with anti-CHC antibody (Ab 24578) prepared in 5% skim milk in assay buffer for 3 hours at RT. Following washes, the membrane was incubated with HRP-conjugated anti-mouse secondary antibody (Jackson 115-035-003) for 1 hour at RT and subsequently probed for bound terminal-domain using a chemiluminescent substrate (West Pico, Thermo).

3.2.3 Pull-down assay

See Methods section 2.2.3 for details.

3.2.4 Cell culture and transfections

Cos7 cells were grown and maintained in DMEM medium (Thermo) supplemented with 10% FBS (Thermo) containing 100 U/mL penicillin and streptomycin (Thermo) in a humidified CO_2 incubator maintained at 5% CO_2 and 37°C.

Cells at 60-70% confluency were transfected with plasmids expressing either GFP-$Numb_{335-554}$ or GFP using Lipofectamine 2000 (Sigma). Briefly, Lipofectamine 2000 (1.5 µl) and plasmid DNA (1 µg) was added to Optimem (Thermo) and incubated at RT for 20 mins. Subsequently the growth medium was replaced with the Optimem mixture. After 4 hours, cells were replated on 40mm glass-coverslips for subsequent live-cell imaging experiments.

3.2.5 Transferrin-uptake assay

Cos7 cells transfected with either GFP-$Numb_{335-554}$ or GFP were grown on 40 mm glass cover-slips. After 36 hours, growth medium was replaced with serum free DMEM and kept

for 2 hours. The coverslip was then assembled in a flow cell (FCS2, Bioptechs) and incubated with 10 μg/ml Alexa594-conjugated human transferrin (Invitrogen) in serum free DMEM for 15 min at 37°C to allow for internalization. Cells were washed with Hanks balanced salt solution (HBSS) and subsequently imaged. To quantitate uptake, transferrin fluorescence was collected and normalized to the area of the cell. Normalized transferrin fluorescence from cells transfected with GFP-Numb$_{335-554}$, GFP, and untransfected cells was compared.

3.2.6 Fluorescence imaging

Cells were imaged on an Olympus IX83 inverted microscope equipped with a 100x, 1.4 NA oil-immersion objective. Fluorescent probes were excited with a stable LED light source (CoolLED pE-4000) and fluorescence emission was collected through filters with excitation/emission wavelength band passes of 472 ± 15 nm/520 ± 15 nm for GFP and 624 ± 20 nm/ 692 ± 20 nm for Alexa594 mCherry probes simultaneously on an Evolve 512 EMCCD camera (Photometrics). Image acquisition was controlled by Micro-Manager [58,59].

3.3 Results

3.3.1 Numb interacts with clathrin via the proline-rich region

Conventionally, CBMs are determined by generating a GST-tagged fragment library of an adaptor, where each fragment is tested for its ability to bind the clathrin terminal domain (CTD) or full-length clathrin [8,44,60]. To determine the clathrin binding region on Numb, a C-terminal deletion library that retained the PTB was generated (Fig 3.1A) and purified using tandem affinity chromatography (See Methods 2.2.1). These deletions were first tested for binding the clathrin terminal domain (CTD) using a rapid and facile dot blot assay. A peptide-overlay assay, similar to the dot-blot assay described here, was previously used to map clathrin-binding sites on AP180 and CALM[61,62]. Briefly, equal amounts of each deletion construct was spotted on a nitrocellulose sheet, incubated with 1μM of the CTD and probed for retained CTD using immunoblotting (See Methods 3.2.2). The PTB domain displayed negligible binding (Fig. 3.1B, C), thus served as a control in these experiments. Importantly, the dot blot assay identified 3 deletions (Δ347-575, Δ545-592 and Δ448-473), which showed significant defects in CTD binding compared to full length Numb (Fig 3.1C, red bars). Interestingly, 2 deletions (Δ184-347 and Δ497-522) bound CTD significantly better than full-length Numb (Fig. 3.1 B, C).

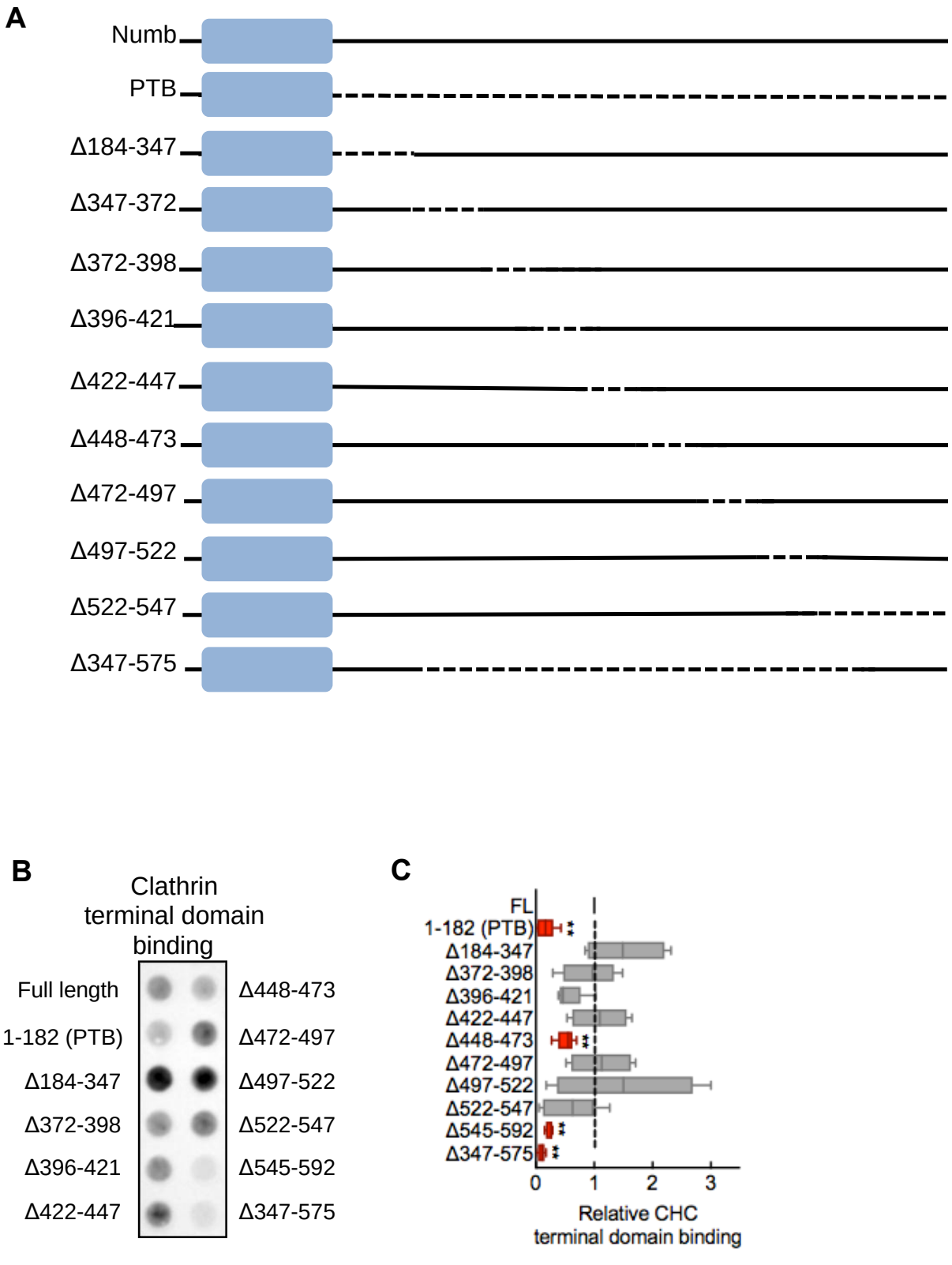

Figure 3.1 A dot-blot screen to identify clathrin-binding attributes on Numb (A) A schematic of Numb deletion constructs. Dotted lines represent the missing stretch in each construct with numbers on the left indicating the residues deleted in each construct. (B) A representative dot-blot with the indicated deletion constructs incubated with clathrin CTD and immunoblotted with anti-CHC antibody. (C) Quantitation of CTD-binding seen with each deletion construct (N=5). Data is normalized to CTD-binding seen with full-length

Numb (FL, dotted line) and represented as box and whisker plot (whiskers represent minimum and maximum values). The constructs showing significant reduction in CTD-binding are highlighted in red. Significance calculated using Mann-Whitney's test.

Despite its utility, the dot-blot assay produced variable results (Fig. 3.1B,C) and could have suffered from low signal-to-noise since the CTD, unlike clathrin, does not self-assemble into lattices. In addition, proteins spotted on nitrocellulose may be organized differently from membrane-bound adaptors. Thus, deletions that showed significant loss in CTD-binding were further tested for clathrin binding when displayed on SUPER templates. Surprisingly, only the longest deletion construct (Δ347-575) showed complete loss while the shorter deletions (Δ448-473 and Δ545-592) showed marginal loss in clathrin binding (Fig 3.2A) and could possibly indicating presence of multiple clathrin-interacting regions.

Conversely, to test if these regions independently define a clathrin-binding motif, they were cloned out and placed downstream of GFP and tested in SUPER template pull down assays (See Methods 3.2.1). Indeed, the region between 347-575 as well as a shorter region 335-554 that falls in between the two AP2-interacting DPF motifs (Fig. 3.2D) recruited clathrin to almost equivalent levels as seen with full-length protein, while residues 448-473 and 545-592 displayed weak binding to clathrin (Fig 3.2 B,C). The region between the two DPFs (335-554) on Numb refered to as the proline-rich region (PRR) [29,63], coincides with the region that binds clathrin (Fig. 3.2D). Together, these results define the clathrin binding site on Numb to be located on the PRR and suggest the possibility that this region harbors multiple clathrin binding sites of weak affinities that come together in the full-length protein and facilitate high avidity interaction with clathrin. Of note, this region was still unable to bind clathrin in brain-extract, possibly due steric interference by the other binding partners.

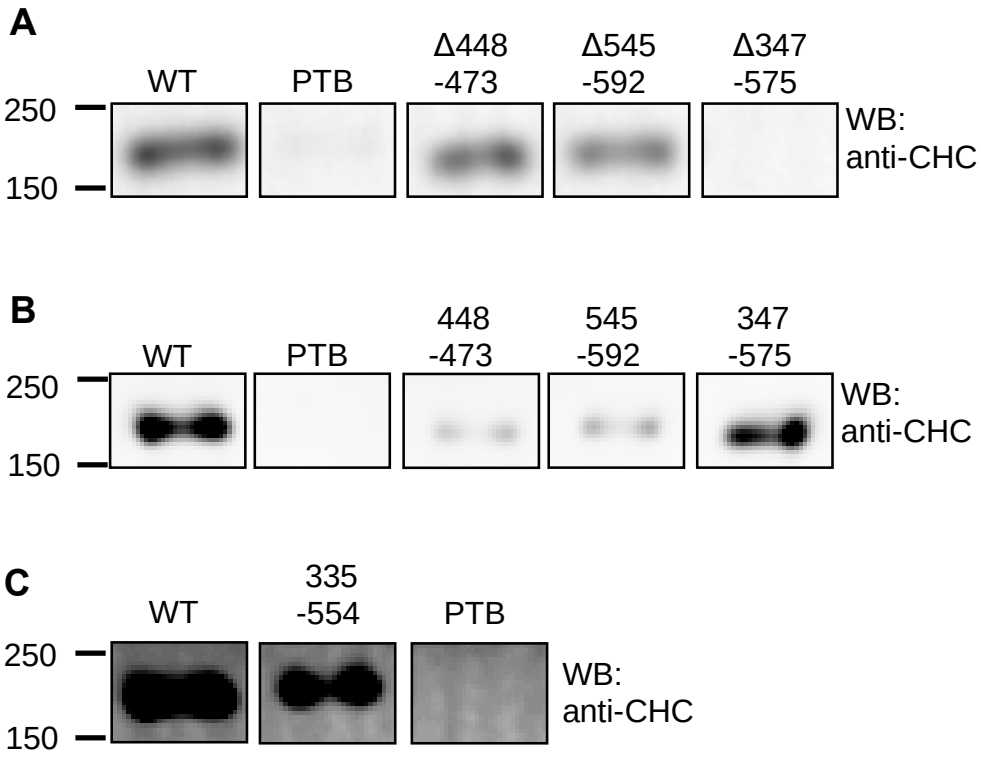

D

P49757 (NUMB_HUMAN) Isoform 4

MNKLRQSFRRKKDVYVPEASRPHQWQTDEEGVRTGKCSFPVKYLGHVEVDESRGMHIC
EDAVKRLKATGKKAVKAVLWVSADGLRVVDEKTKDLIVDQTIEKVSFCAPDRNFDRAF
SYICRDGTTRRWICHCFMAVKDTGERLSHAVGCAFAACLERKQKREKECGVTATFDAS
RTTFTREGSFRVTTATEQAEREEIMKQMQDAKKAETDKIVVGSSVAPGNTAPSPSSPT
SPTSDATTSLEMNNPHAIPRRHAPIEQLARQGSFRGFPALSQKMSPFKRQLSLRINEL
PSTMQRKTDFPIKNAVPEVEGEAESISSLCSQITNAFSTPEDPFSSAPMTKPVTVVAP
QSPTFQGTEWGQSSGAASPGLFQAGHRRTPSEADRWLEEVSKSVRAQQPQASAAPLQP
VLQPPPPTAISQPASPFQGNAFLTSQPVPVGVVPALQPAFVPAQSYPVANGMPYPAPN
VPVVGITPSKMVANVFGTAGHPQAAHPHQSPSLVRQQTFPHYEASSATTSPFFKPPAQ
HLNGSAAFNGVDDGRLASADRHTEVPTGTCPVDPFEAQWAALENKSKQRTNPSPTNPF
SSDLQKTFEIEL

Figure 3.2 Numb PRR independently interacts with CHC (A) Western blot showing CHC-recruited by different deletions of Numb. Δ347-575 shows complete loss in CHC-binding. (B) Deleted residues from (A) were tested for their ability to independently bind CHC. Numb$_{347-575}$ displays most efficient binding to CHC. (C) The region between the two DPFs, Numb $_{335-554,}$ defined as the PRR is sufficient to interact with CHC. (D) Sequence of Numb (isoform 4). PRR is marked in red. DPF sites that link Numb and AP-2 are marked in green.

3.3.2 Overexpression of Numb PRR perturbs transferrin trafficking

Overexpression of the clathrin-binding domains of several adaptors has been reported to act as dominant-negative to CME by sequestering clathrin and AP-2[6,64]. To analyze the significance of the Numb-clathrin interaction, trafficking of the transferrin receptor (TfR), a model cargo for CME, was analyzed in COS-7 cells overexpressing GFP-tagged Numb PRR. TfR is endocytosed by clathrin-mediated pathways and subsequently enters the early endosomes. From the early endosomes, it is transported back to the cell surface via the fast, Rab4a-dependent and the slow, Rab4b-dependent recycling pathways. Both the Rab4b and Rab4a recruit clathrin via AP1 and GGA3 to facilitate recycling [65,66]. The bulk of TfR at steady-state is localized in recycling endosomes and thus marks this compartment.

To monitor effects on transferrin uptake, cells were serum starved and incubated with fluorescently-labeled human transferrin (See Methods 3.2.5) for 15 mins, washed and then imaged. Compared to non-transfected cells that showed intense signal at the perinuclear recycling endosome compartment, cells expressing GFP-Numb PRR showed dramatically reduced uptake of fluorescent transferrin (Fig 3.3A). Quantitation across multiple cells and experiments revealed that transfected cells showed ~50% lower fluorescent transferrin signal compared to non-transfected cells (Fig. 3.3B). Previous results indicate that overexpression of the Numb 335-554 (PRR) inhibits CME in cells, although mechanisms that cause this effect have remained unexplained[20]. Considering that both the early endosomes and the plasma membrane recruit clathrin from a common cytosolic pool, these results may indeed be explained by depletion of clathrin due its binding to Numb PRR. The possibility that Numb PRR may be recruiting additional factors integral to vesicle-transport remains.

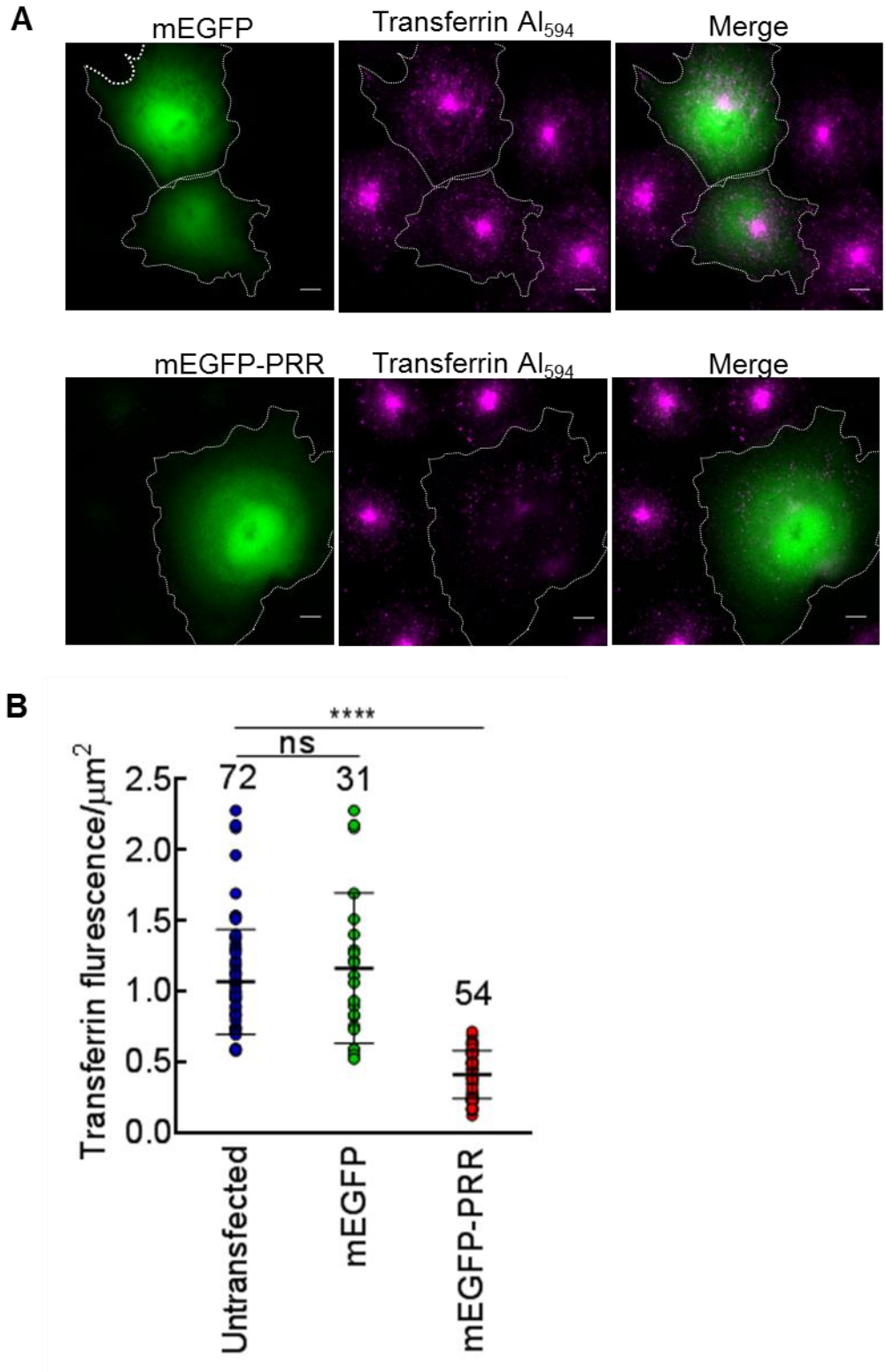

Figure 3.3 Overexpression of Numb-clathrin binding domain impairs transferrin trafficking (A) Epifluorescence images of transferrin uptake in COS-7 cells expressing GFP-Numb$_{335-554}$. (B) Transferrin intensity per μm^2 from (A) N=3, n≥30. Significance calculated using Mann Whitney's test.

3.4 Discussion

A combination of dot-blot assay and pull-downs with membrane-displayed deletions of Numb described here identified Numb PRR (Numb 335-554) to be integral for clathrin-binding. Numb PRR on its own is sufficient to interact with clathrin. Further, two separate deletions (Δ448-473, Δ545-592) spanning the PRR region show a significant loss in CTD-binding in the dot-blot assay. Surprisingly, both Δ448-473 and Δ545-592 are not defective in binding clathrin heavy chain in a SUPER template pull-down (Fig 3.2A). Both these regions when cloned out individually and tested in pull-down assays display weak binding to clathrin heavy chain. Almost all of the adaptors known till date need multiple CBM to polymerize clathrin effectively. It is indeed surprising that narrowing down the Numb PRR to pin down the CBM/s did not yield conclusive results (Fig 3.1, 3.2). While CBMs of most adaptors are on their own sufficient to bind clathrin, some adaptors need larger portions of their C-terminal tails to assemble clathrin effectively. Adaptor-protein ARH, responsible for endocytosis of LDLR (low-density lipoprotein receptor), needs the residues between the region 180-308 on its C-terminal tail for efficient clathrin-binding [8]. The C-terminal ~16 kDa sub-domain in AP180 (which has relatively high similarity with CALM) has been reported to mediate clathrin-assembly; while mutations in the DLL/DLF motifs have negligible effect on clathrin binding ability [61,62].

Curiously, overexpression of the fragment of Numb PRR in COS-7 cells showed a block in transferrin-uptake. Similar overexpression of several endocytic-adaptors have been reported to act as dominant negative to clathrin-mediated endocytosis, presumably by sequestering essential coat components. Overexpression $Numb_{335-554}$ leading to a block in transferrin uptake may be explained by several mechanisms- 1) block in endocytosis of transferrin due to depletion of clathrin, 2) block in recycling of TfnR from the recycling endosomes, and 3) inhibition in endocytosis of transferrin due to TfnR receptor being accumulated in the recycling endosomes. Interestingly, a recent study identified that Numb PRR recruits the small GTPase Rab7 to the early endosomes[21]. Rab7 acts as a switch that promotes early to late endosomal transformation[67,68] and the early endosomes are enlarged in absence of Rab7. Indeed the inhibiton of transferrin uptake upon Numb PRR overexpression could also be a consequence of sequestration of Rab7. Independently, in order to test if overexpression of Numb PRR causes a block in CME by sequestering clathrin, surface densities of clathrin-coated pits can be analysed.

Recently, Numb isoform that vary in the PRR (p66 and p72) were seen to regulate the balance between receptor recycling and degradation from the early endosomes, presumably by recruiting different partners [69]. Indeed, it would be of interest to analyse if the Numb-clathrin interaction is conserved between the different Numb isoforms.

Chapter 4

Determinants of membrane-binding and the membrane-active nature of Numb

4.1 Introduction

Clathrin-mediated endocytosis is the central pathway that mediates transport of cargo proteins from cell surface to the interior, clathrin being the key player [70]. However, clathrin does not bind directly to the membrane or the cargo receptors and relies on cargo-adaptor proteins for its recruitment [3]. These adaptor proteins are also cytosolic and are transiently recruited to the target membrane either by binding to a specific phospholipid or the cytosolic cargo-tail[12]. Anionic phosphoinositide PIP_2 that is enriched at the plasma membrane has been thought to aid the recruitment of AP-2, as well as other monomeric adaptor proteins. Depletion of PIP_2 from the plasma membrane leads to a loss of clathrin-coated pits and dissociation of adaptor proteins from the membrane[71]. Similarly, deletion of sorting motifs from cytosolic domains of several transmembrane cargo receptors has been shown to hamper their endocytosis. Thus, the coincident detection of specific phospholipid and the cognate cytosolic cargo-tail is required for recruitment of adaptor proteins to their target membranes.

Numb directly binds cargo proteins containing the conserved NPxY motif. Positively charged residues in the PTB domain of Numb are thought to mediate its recruitment to negatively charged membranes. Pull-down using SUPER templates described here report a direct interaction between Numb and clathrin (See Fig 2.5). To visualize the process of Numb-mediated clathrin assembly on membranes, factors to recruit Numb onto the membranes are first determined. To this end, cargo and lipid-binding properties of Numb are employed to aid its recruitment onto the membranes.

4.2 Methods

4.2.1 Cloning, protein expression, and purification

Human Numb (Isoform 4, Open Biosystems plasmid # 5217787) was cloned into pET15B with N-terminal 6xHis-tag and C-terminal StrepII tag. 6xHis-TEV-Numb-mEGFP-StrepII was generated by inserting mEGFP between Numb and StrepII. Numb-mEGFP-StrepII was made by deleting 6XHis and TEV from 6xHis-TEV-Numb-mEGFP-StrepII. Numb PTB (residues 1-183) was generated by deleting the C-terminal tail. PTB Swap was made by inserting Dab2 PTB (P98078: Isoform p96) in place of Numb PTB. 6X-His-TEV-NPC1L1 C-tail (1266-1332)-StrepII was generated by cloning the cytosolic domain of NPC1L1 (Open Biosystems clone MHS6278-211691094) with 6xHis and StrepII tags at the N- and C-terminii. Mouse Dab2 (P98078: Isoform p96) was also cloned with 6xHis and StrepII tags at

the N- and C-terminii. All constructs were generated by PCR-based seamless cloning and confirmed by sequencing. All proteins were recombinantly expressed and purified as described in Methods 2.2.1. NPC1L1 (1266-1332) was expressed in BL21(DE3) and protein expression was induced by 0.1mM IPTG, at room temperature for 3 hours. The lysate was incubated at 75°C for 30 mins, cooled rapidly and centrifuged. The protein in the supernatant was purified by affinity chromatography using the 6xHis and StrepII tags.

For long-term storage (3 months) proteins were stored in buffer (20mM HEPES pH7.4, 150mM NaCl, 1mM DTT, 10% glycerol), flash frozen in liquid nitrogen and stored at -80°C.

4.2.2 Lipid dot blot

Stocks of all lipids were reconstituted in choloform to the final concentration of 1 mM. 1 nm of each of the lipid was spotted onto nitrocellulose membrane and incubated with blocking buffer (3% fatty-acid free BSA in 20 mM HEPES-KOH, pH 7.4, 150 mM KCL) for 1hr at room temperature. Numb (1 μM) was added to the blocking buffer and incubated at RT for 3 hours followed by washing with HKS. Blot was immersed in 1μg/ml of Streptavidin-$Alexa_{488}$ conjugate prepared in HKS and incubated for an hour with gentle shaking followed by washes with HKS. The images were captured using green filters on LAS-4000 (GE). Intensity of bound Numb for each lipid was calculated by placing an ROI on the signal. Background intensity was subtracted from fluorescence intensity for each lipid. To obtain the relative binding of Numb to lipids, all the intensities were normalized to the lipid with the highest intensity.

4.2.3 SMrT templates

SMrTs were prepared as described earlier[72]. Briefly, lipid stocks (Avanti Polar Lipids) were aliquoted into glass vials in required proportions, diluted to a final concentration of 1 mM total lipid in chloroform and stored at -80 °C. p-Texas Red-DHPE isomer was separated from a mixed isomer stock of Texas Red DHPE (Invitrogen) using thin layer chromatography on silica gel plates (Sigma) against 100% methanol as described earlier [73]. Lipid stocks were brought to room temperature before use. A small aliquot (~1-5 nmol total lipid) was spread on a freshly cleaned PEGylated coverslip and kept under high vacuum for 5 min to remove all traces of chloroform. A ~35 μl flow cell (Bioptechs) was assembled by placing a 0.1 mm silicone spacer between the PEGylated coverslip and an ITO-coated slide. The flow cell was filled with filtered and degassed HKS left undisturbed for 10 min at room temperature.

Supported membrane tubes (SMrT) were created by extrusion of the large vesicles, formed during hydration, to narrow membrane tubes by flowing excess HKS at high (~30 mm/s particle velocity inside the chamber) flow rates. SMrT templates were judged ready for experiments when the entire membrane reservoir was extruded into tubes that remained pinned at discrete sites to the surface.

All lipid mixes are made with DOPC, DOPS and *para*-TexasRed DHPE (79:15:1 mol%) along with the addition of either $DOPIP_2$ or DGSNTA(Ni^{2+}) (both at 5mol%).

4.2.4 Fluorescence imaging

Fluorescence imaging was carried using an Olympus IX71 inverted microscope through a 100X, 1.4 NA oil-immersion objective. LED light source (Thorlabs) was used to excite fluorescent probes, and emitted fluorescence collected using single-band pass filters (Semrock) with excitation/emission wavelength bandpasses of 482±35 nm/536 ± 40 nm for mEGFP, 562±40 nm/624±40nm for Texas Red, and 628±40 nm/692±40nm for DiD probes on an Evolve 512 EMCCD camera (Photometrics). Image acquisition was managed by the MetaMorph soft-ware (Molecular Devices).

4.3.5 Image analysis

Image analysis was carried out using Fiji [74]. Statistical analysis was carried out using Graphpad prism (version 5.0a).

4.3 Results

4.3.1 Characterization of Numb-lipid binding

To recreate the process of Numb-mediated clathrin assembly on membrane surface, determinants of Numb-membrane recruitment were first analysed. To this end, intrinsic lipid-binding preferences of Numb were tested using a fat-blot assay. Recombinantly expressed full-length Numb was purified using the N-terminal 6xHis and C-terminal StrepII tags. Of note, unlike the other clathrin adaptors purified using tandem affinity-tag method, Numb purified in association with lower molecular degradation products (data not shown). Inclusion of high salt washes prior to elution from the Stepactin column eliminated these degradation products (Fig 4.1A). To test for lipid-specificity, equal amounts of various phospholipids were spotted on a nitrocellulose membrane, blocked with 3% BSA and incubated with purified Numb. Protein binding was detected using fluorescently-tagged streptavidin that

bound the StrepII tag (Fig 4.1B). Biotinylated PE served as control showing maximum binding to streptavidin. Numb promiscuously associated with all acidic-phospholipids showing only marginally higher binding to PI3P (Fig 4.1C). This is in agreement with liposome sedimentation assays done with the PTB domain of Numb [75]. Phosphatidylinositol 4,5-bisphosphate (PIP_2), the central regulator of CME enriched on the plasma membrane, is chosen to study Numb function of membranes.

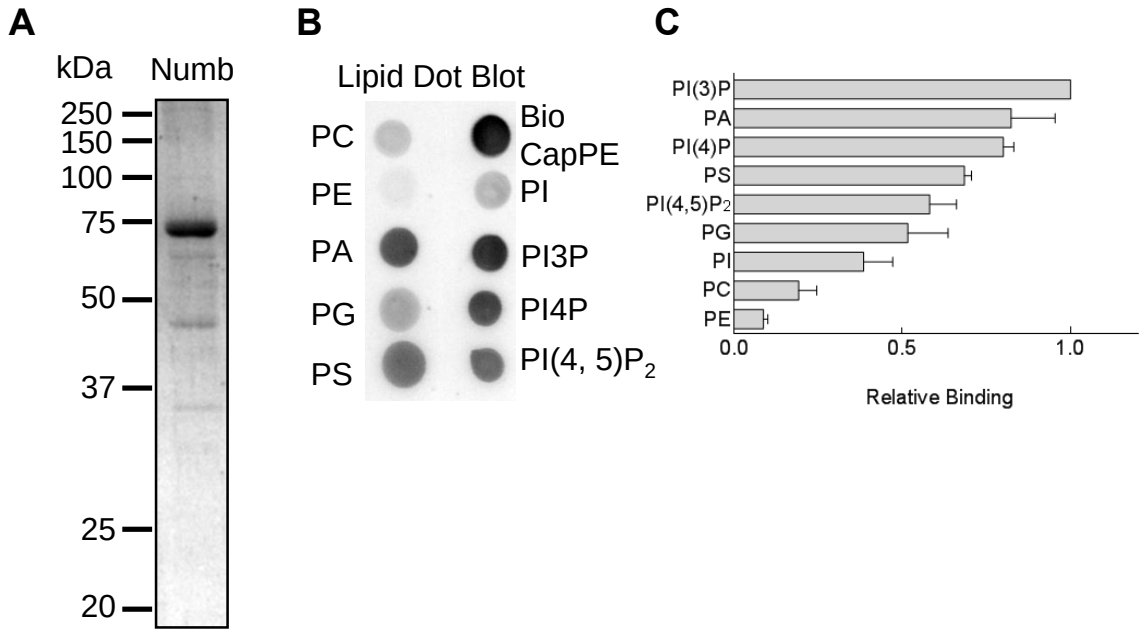

Figure 4.1 Numb binds acidic phospholipids (A) 10% coomassie-stained SDS PAGE gel of Numb purified using affinity chromatography (B) Representative image of fat blot showing Numb binding to an array of phospholipids. Fluorescently-labelled streptavidin that recognizes StrepII tag was used to report Numb binding (C) Quantitation of fat blot (N=3) showing relative binding of Numb to various lipids.

4.3.2 SMrTs mimic topological intermediates in clathrin-coated vesicle formation

Molecules involved in making a clathrin-coated vesicle sample a large range of membrane curvatures, starting from a relatively planar donor-membrane which is reshaped into a shallow pit and then a highly-curved bud that remains connected to the donor membrane via a thin neck. SMrTs [45,76] consisting of a planar bilayer and membrane-tubes displaying a wide range of radii mimic distinct topological stages of a maturing CCV (Fig 4.2 A). In addition, given that the tubes sizes are diffraction-limited, changes in tube fluorescence directly correlate to changes in tube dimensions[77]. Sizes of membrane tubes can therefore be arrived at from their fluorescence intensities by an *in situ* calibration method as described earlier[10] and typically fall from 10-50 nm of radius. Briefly, images of the Supported Lipid

Bilayer (SLB) for each SMrT experiment were acquired and background corrected. Integrated fluorescence intensity (IFI) was estimated in various regions of interest (ROIs) of different sizes placed on SLB. Calibration constant (K1, slope of the graph) was estimated by plotting IFI of different ROIs against their respective areas. Images of tubes were background corrected; integrated fluorescence intensity (IFI) was estimated by placing ROIs of length (l) on different tubes. Next, IFI of tube was converted into membrane area by dividing it by K1, this membrane area was converted to tube radius (r) using equation r = membrane area $(2\pi * l)^{-1}$. A scaling factor was generated to equate maximum pixel intensity on the tube to its radius. In order to do this maximum pixel intensity along the tube was plotted against its radius (r) to get second calibration constant (K2) (slope of the plot). Radius of the tube can now be obtained by dividing maximum pixel intensity on the tube by K2 (Fig 1B).

Adaptor proteins often recognize their target membrane by detection of both, a specific lipid and membrane-associated proteins [78,79]. In order to recruit Numb, SMrTs are functionalized by the inclusion of a small amount of the acidic phospholipid PIP_2 (5mol%). SMrTs are made as described in Methods 4.2.3. Using PLCδPH, a PIP_2 specific marker[80], PIP_2 distribution on supported lipid bilayers (SLB) and tubes was found to be uniform (Fig 4.2 B and C). Apart from PIP_2, Numb also associates with membranes by recognizing specific motifs on cytosolic domains of trans-membrane receptor proteins. The cholesterol receptor NPC1L1 is the well-studied cargo for Numb and contains the characterized Numb-binding motif [19] in its cytosolic domain. A minimal cargo mimic designed using the cytosolic tail (residue number 1266-1332) of the cholesterol receptor NPC1L1 fused to a hexahistidine tag was therefore used to facilitate Numb recruitment (Fig 4.2 D) (referred to as $NPC1L1_{(1266-1332)}$ for simplicity). SMrTs were doped with chelating lipid (5mol% DGS NTA(Ni^{2+})) to facilitate display of $NPC1L1_{(1266-1332)}$.

A

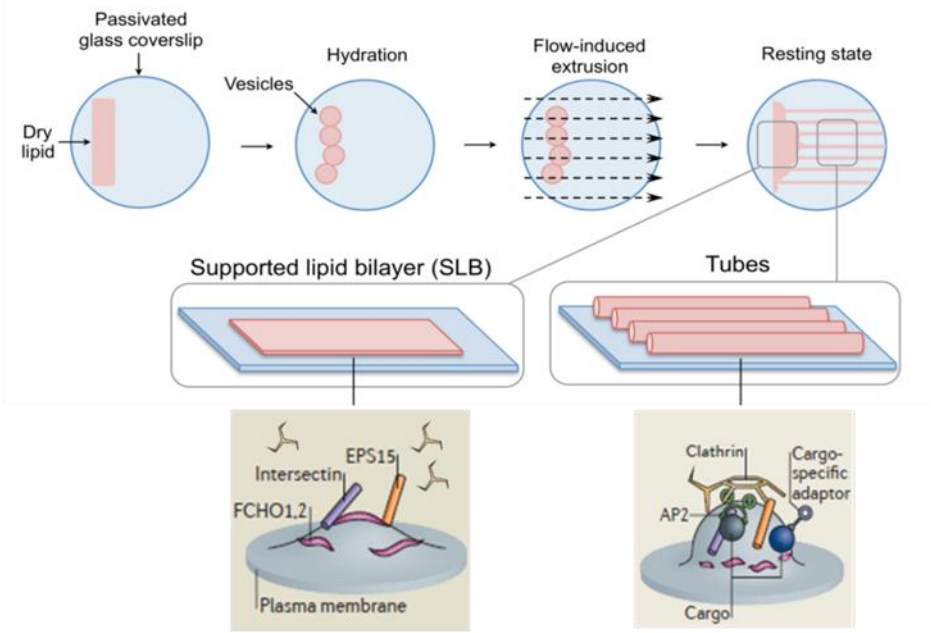

B

Step1
Images of supported lipid bilayer (SLB) were acquired and background corrected.Integrated fluorescence intensity (IFI) was estimated in various regions of interest (ROIs) of different sizes placed on SLB

Step 2
Calibration constant (K1, slope of the graph) was estimated by plotting IFI of different ROIs against their respective areas

Step 3
Images of tubes were background corrected; integrated fluorescence intensity (IFI) was estimated by placing ROIs of length (l) on different tubes.

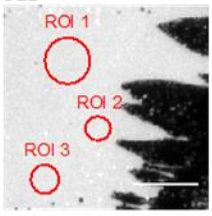

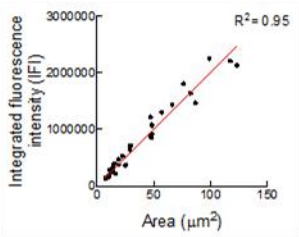

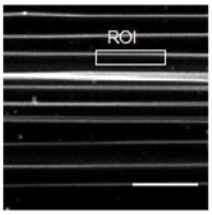

Step 4
IFI of tube was converted into membrane area by dividing it by K1, this membrane area was converted to tube radius (r) using equation r = membrane area $(2\pi^*l)^{-1}$

Step 5
The maximum pixel intensity along the tube was plotted against its radius (r) to get second calibration constant (K2) (slope of the plot)

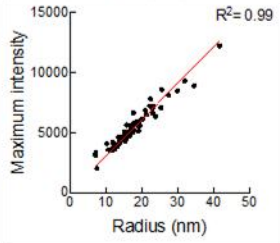

Step 6
Radius of the tube can be obtained by dividing maximum pixel intensity on the tube by K2.

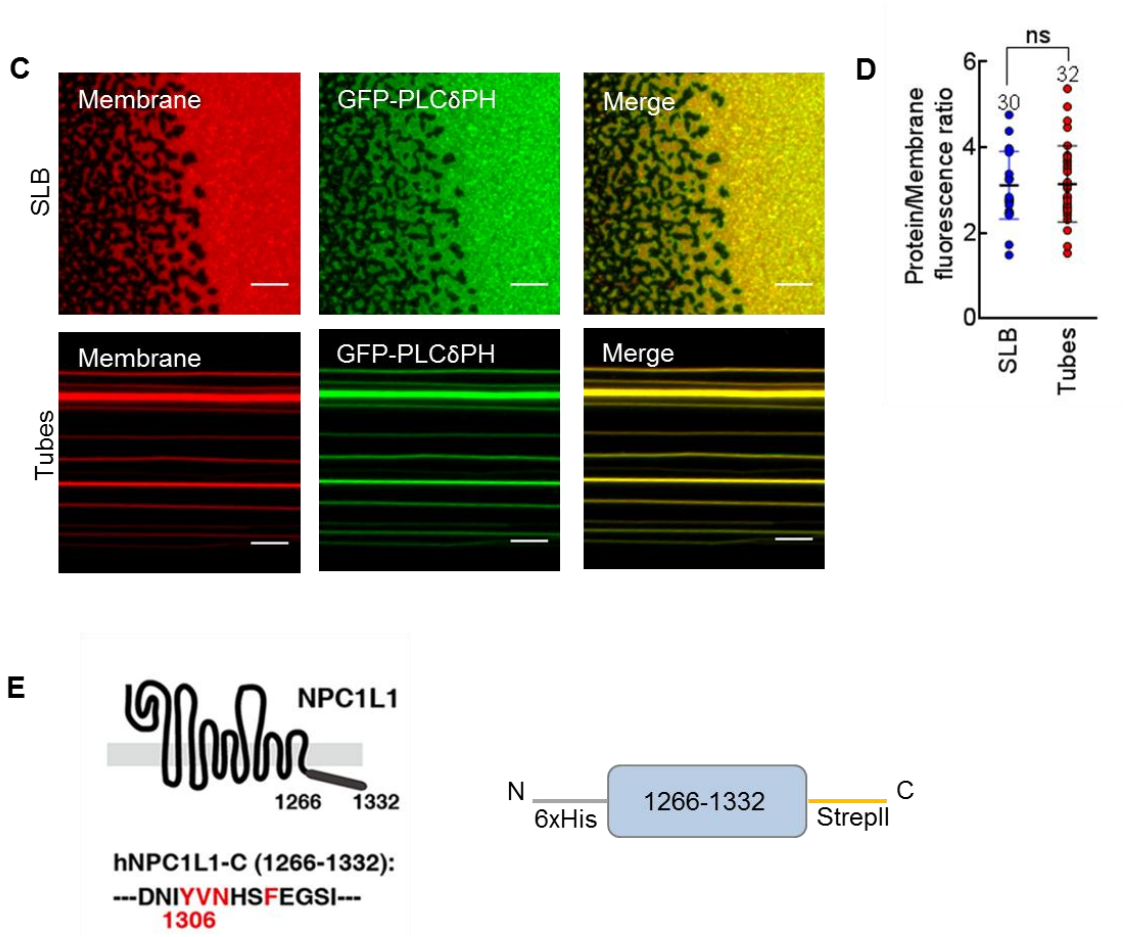

Figure 4.2 Supported membrane tube (SMrT) represent varying membrane curvatures found during CCV formation (A) Schematic of SMrT Template assay. Supported lipid bilayer (SLB) mimics planar bilayer found at the start of forming a CCP while tubes mimic bud/curved intermediates of a maturing CCP (Adapted from [70,72] (B) Schematic of tube radius estimation. (C) Representative fluorescence micrographs showing distribution of mEGFP-PLCδPH on SLBs and tubes. (D) Analysis of protein to membrane fluorescence ratio from (C) shows equal mEGFP-PLCδPH densities on SLB and tubes. Number of tubes ans SLbs analysed are indicated on the top of each dataset. (E) Schematic of the cholesterol receptor NPC1L1 (Reproduced from [19]) and the design for mimic of Numb's cargo-the transmembrane receptor NPC1L1 cytosolic domain fused to N-terminal hexahistidine tag.

4.3.3 Cargo and lipid-aided organization of Numb on membrane

To visualize membrane-binding, the C-terminus of Numb was fused to mEGFP. C-terminally tagged Numb is reported to be functionally active in cell-fate determination in *drosophila* embryos[32]. Purified Numb-mEGFP was incubated with SMrTs containing PIP_2. Within minutes, Numb-mEGFP bound and coated the membrane tubes. Surprisingly, Numb showed negligible binding to the planar SLBs (Fig 4.3A, D), suggesting an intrinsic preference for PIP_2-mediated binding to regions of high membrane-curvature. Moreover,

Numb fluorescence was non-uniform and arranged as discernible, separate clusters. This is in clear contrast to PIP_2-recurited PLCδPH which uniformly coats membrane tubes and SLBs (Fig 4.2B). Notably, not all tubes showed non-uniformed, clustered Numb-mEGFP distribution, a phenomenon that was found to be a function of starting tube dimension (as described in 4.3.4).

Numb also bound to membranes displaying NPC1L1 $_{(1266\text{-}1332)}$ (Fig 4.3B). Briefly, SMrTs containing chelating lipid were incubated with purified NPC1L1 $_{(1266\text{-}1332)}$. To avoid it from binding Numb-mEGFP in solution, excess unbound NPC1L1 $_{(1266\text{-}1332)}$ was first washed and then Numb-mEGFP was flowed-in, incubated and imaged. Surprisingly, curvature dependent binding was over-ridden when NPC1L1 was used to recruit Numb, and clusters of protein were seen on both SLB and tubes (Fig 4.3B, D). Of note, the clusters on tubes were not as tight as those observed with PIP_2-recruited Numb.

Numb recruitment is completely dependent on the presence of either PIP_2 or NPC1L1 $_{(1266\text{-}1332)}$ with no protein binding observed on templates containing just DOPC and DOPS (Fig 4.3C).

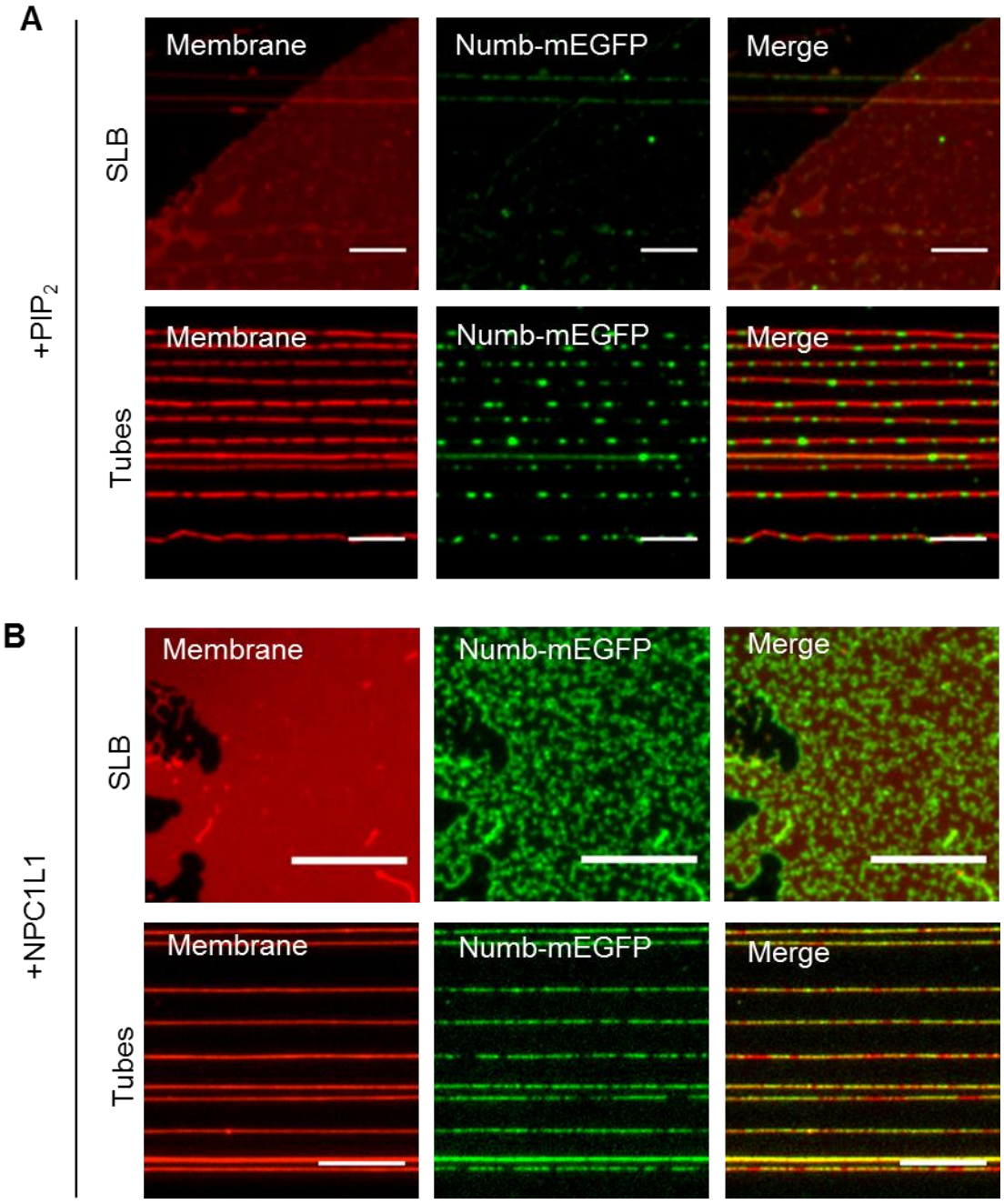
A
+PIP2
SLB
Membrane
Numb-mEGFP
Merge
Tubes
Membrane
Numb-mEGFP
Merge
B
+NPC1L1
SLB
Membrane
Numb-mEGFP
Merge
Tubes
Membrane
Numb-mEGFP
Merge

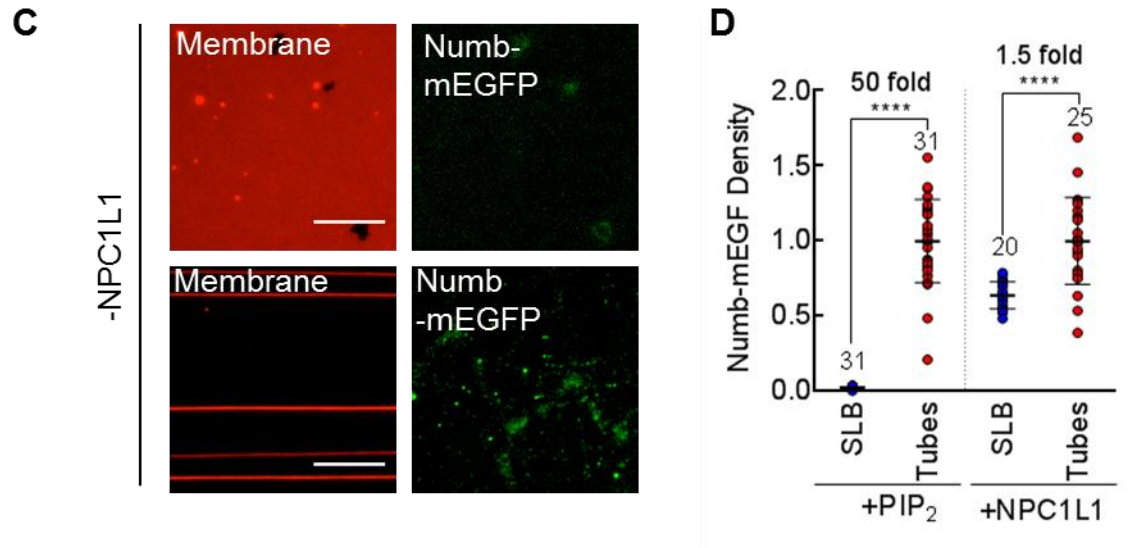

Figure 4.3 Mode of recruitment dictates Numb organization on membranes (A) Numb-mEGFP shows curvature dependent-binding to SLB and tubes containing PIP_2 (5mol%) and is organized as distinct clusters on tubes. (B) NPC1L1 recruits Numb-mEGFP to SLB as well as tubes. Numb-mEGFP organised as distinct clusters on both SLB and tubes (C) Numb does not bind membranes in absence of NPC1L1 or PIP_2. Scale bar 5µm (D) Quantitation of (A) and (B), significance calculated using Mann Whitney's test. Number of tubes ans SLbs analysed are indicated on the top of each dataset. Scale bar-5µm.

4.3.4 Numb oligomerization drives membrane-remodeling

Interestingly, the tube underneath Numb clusters showed dramatic membrane remodeling with regions of alternating high and low membrane fluorescence (Fig 4.4A). The fluorescence intensity profile of one such single tube reveals that regions of high Numb-mEGFP intensity coincide with regions of low membrane intensity suggesting that Numb clusters constrict the underlying tube. Epsin1, clathrin adaptor reported to bind PIP_2 with high affinity, coated all tubes uniformly and did not lead to changes in tube fluorescence (Fig 4.4B). Pull-down-based studies suggest that Numb can dimerize[21]. The clustered, non-uniform distribution may be indeed be a reflection of higher-order oligomers of Numb.

The ability of Numb to form oligomers seem to be dependent on the initial tubes diameter with tubes of higher membrane florescence intensity showing uniform Numb-mEGFP distribution and no membrane remodeling events (Fig 4.4C). In order to systematically analyse such a co-relation, the coefficient of variance (COV) of Numb-mEGFP, an indicator of the extent of clustering, was plotted against starting tube radius (Fig 4.4D). Tubes higher than 20 nm in radius displayed a steep drop in COV values. Similarly, the probability of tube constriction when plotted against the starting tube radius (Fig 4.4E)

also shows a sharp decline after 20 nm of tube-radius. Together these results suggest that- 1) Size of the membrane tube determines organization of Numb with tubes less than 40nm in diameter showing clustered Numb distribution, 2) Formation of Numb-clusters in-turn leads to tube-constriction. Such a size threshold could possibly indicate limitations on oligomeric-arrangement of Numb. More importantly, these results establish the ability of Numb to sense as well as generate curvature. As noted earlier NPC1L1 $_{(1266\text{-}1332)}$-recruited Numb did not show such tightly clustered distribution and produced very faint constrictions on tubes (compare tubes in Fig 4.3 A and B). As the cargo would place Numb farther from the membrane, this difference could possibly reflect differences in the organization of Numb dependent on its proximity from the membrane.

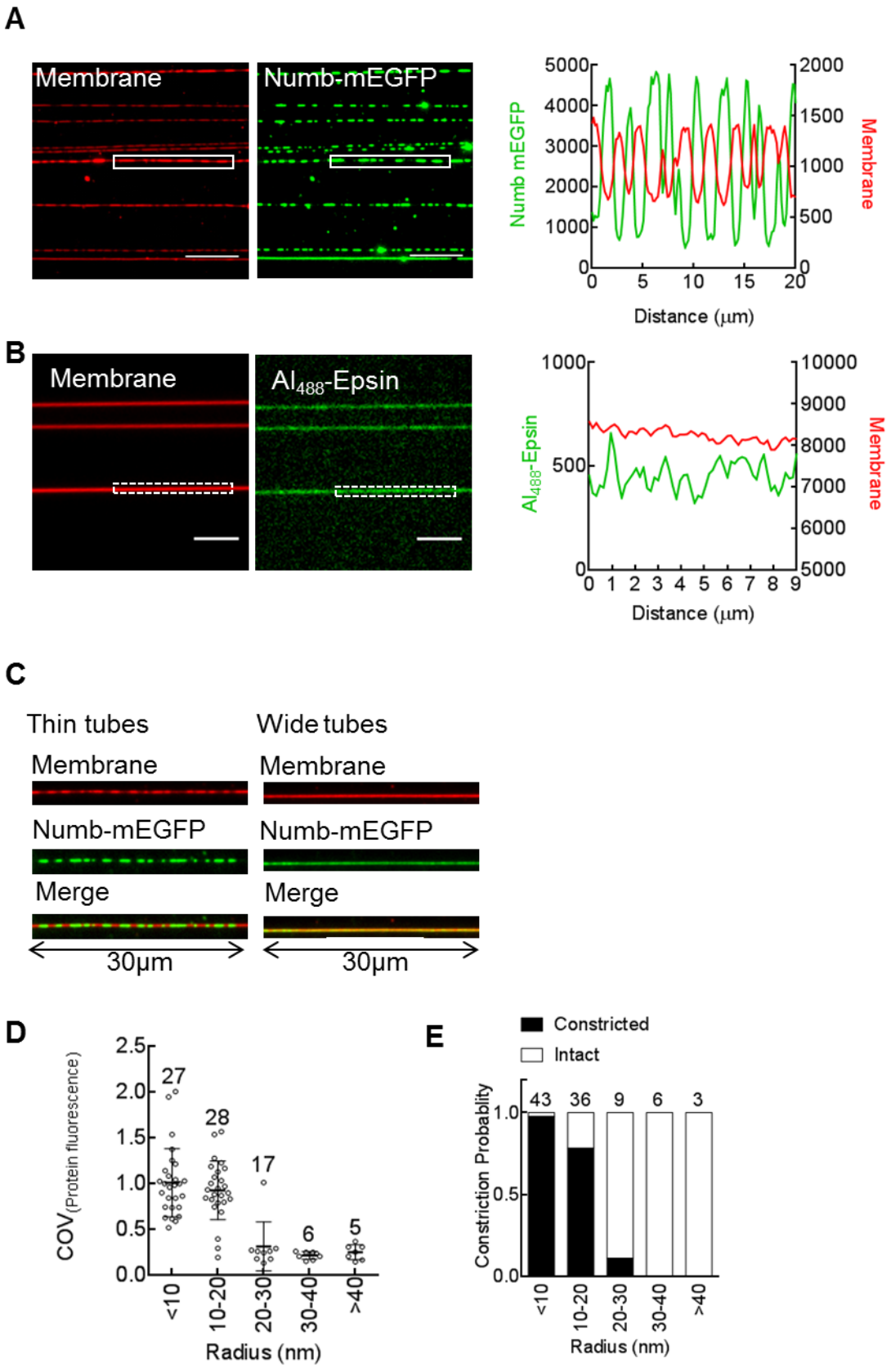

Figure 4.4 Numb oligomers are membrane-active (A) Numb-mEGFP is organized as clusters on tubes containing PIP_2. Membrane underneath clusters is constricted (low tube fluorescence). (B) In contrast epsin1, a

previously reported adaptor that binds PIP_2 with high affinity, coats tubes uniformly. (C) Two types of tubes seen-thin tubes with Numb clusters that coincide with constrictions and wide tubes with uniform Numb distribution that show no membrane-remodeling. (D) Scatter plot showing COV (ability of Numb to form clusters) is dependent on starting tube radius with. Number of tubes analysed are indicated on the top of each dataset. (E) Ability to form clusters in turn dictates probability of constriction. Scale bars-5µm. n≥70 tubes from 2 independent experiments are analysed.

4.3.5 Oligomerization is an intrinsic ability of Numb

Binding to specific lipids has been shown to promote membrane-remodeling activity in proteinS. However, Numb's tendency to oligomerize and remodel tubes appears to be independent of PIP_2 since Numb recruited via its N-terminal hexahistidine tag to chelating lipid containing membranes also showed similar organization. While purified mEGFP uniformly painted SLBs as well as tubes (Fig 4.5A and D top panels, line profile in B and E), Numb-mEGFP showed distinct clusters on membranes (Fig 4.5A and D bottom panels, line profile in C and F). Tubes showed regions of constrictions co-localizing with Numb oligomers (Fig 4.5 D bottom panel, line profile in F). To understand how Numb organizes as clusters 200nM Numb-mEGFP was flowed in on SMrTs containing chelating lipids and imaged in real time. Upon recruitment, Numb-mEGFP distribution was initially uniform and started to show separate clusters in about two minutes with distinct punctae of protein built within 10 minutes (Fig 4.5G); possibly indicating that membrane-localization increases the local concentration of protein facilitating self-organization to form scaffolds.

Recruitment of Numb via N-terminus hexahistidine tag mimics the native orientation of Numb relative to the membrane. Such organization of artificially recruited Numb emphasizes its intrinsic tendency to oligomerize. Furthermore, chelating lipid-based protein recruitment ensures similar membrane densities allowing comparison of membrane organization and clathrin-assembly properties of Numb with other adaptors

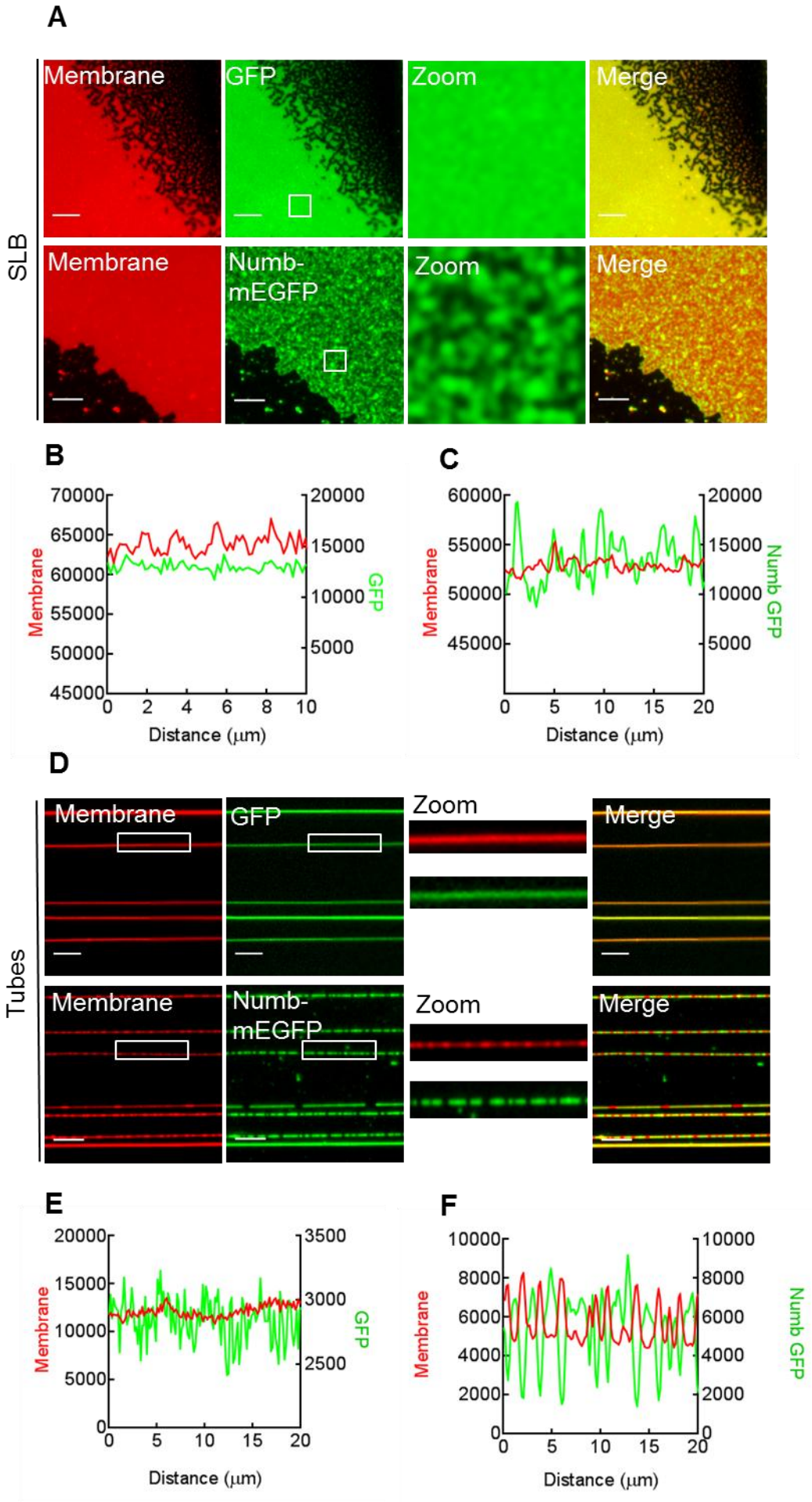
A
SLB
Membrane
GFP
Zoom
Merge
Membrane
Numb-
mEGFP
Zoom
Merge
B
Membrane
GFP
Distance (μm)
C
Membrane
Numb GFP
Distance (μm)
D
Tubes
Membrane
GFP
Zoom
Merge
Membrane
Numb-
mEGFP
Zoom
Merge
E
Membrane
GFP
Distance (μm)
F
Membrane
Numb GFP
Distance (μm)

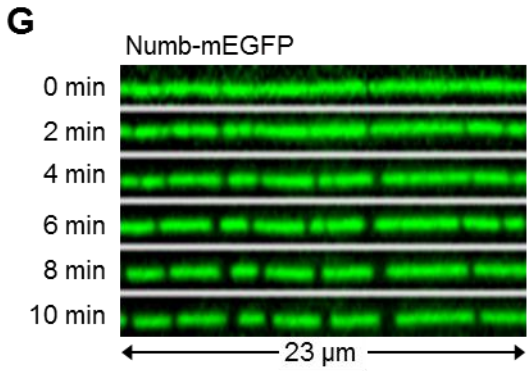

Figure 4.5 Numb has an intrinsic tendency to oligomerize (A) Numb-mEGFP is non-uniformly organized into clusters on SLBs containing CL (5 mol%) (line profile in C) while GFP (top panel) uniformly paints SLBs (line profile in B). (D)Array of tubes containing CL (5 mol%) displaying Numb-mEGFP (bottom panel, line profile in (F)) or GFP (top panel, line profile in E). (G) Time lapse showing formation of Numb-mEGFP clusters on tubes.

4.3.6 Numb PTB domain is sufficient to form clusters

ARH, Dab2 and Numb constitute the PTB-domain containing CLASPs (Clathrin-Associated Sorting Proteins). To investigate the mechanism of Numb-mediated membrane-remodeling, purified Numb and Dab2 were artificially recruited to membranes, thereby allowing their display at equal protein densities, and compared for their abilities to remodel membranes. While Numb produced the signature dramatic constrictions; Dab2 caused no change in membrane fluorescence. Further, since Numb engages with membranes via the PTB domain, purified Numb-PTB was tested and found to be sufficient to cause constrictions on membrane tubes. Moreover, replacing the PTB domain in full-length Numb by the Dab2 PTB (PTB Swap) impaired this property of tube-constriction (Fig 4.6A). Extent of membrane-remodeling for all the proteins was quantified using the COV of tube-fluorescence (Fig 4.6 B). To visualise the protein-organisation on membranes Fluorescently labelled PTB domain was used. Like full-length Numb, PTB domain was arranged as clusters on SLB and tubes. The constrictions on tubes co-localized with clusters of Numb-PTB (Fig 4.6C).

Interestingly, as compared to the full length Numb, the PTB domain formed much smaller clusters and constrictions. Of interest, excessive labeling of cysteine residues with Al_{488}-maleimide was found to hamper oligomerization and membrane-remodeling activities of the PTB domain. The degree of labeling was therefore restricted to only 10% of the protein concentration. Location of critical cysteine residue/s could possibly point to the oligomerization interface on the PTB domain.

Together these results establish that the PTB domain of Numb is sufficient to form oligomers that lead to membrane-remodeling.

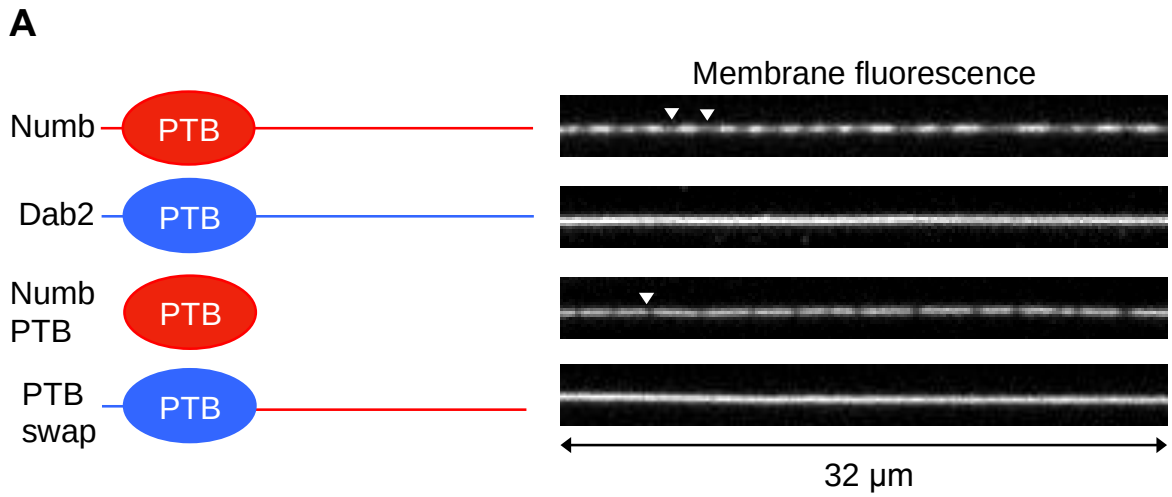

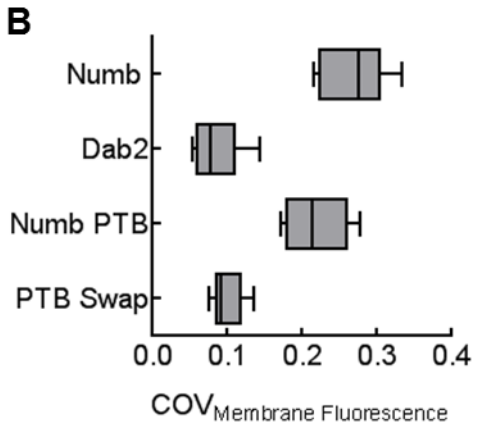

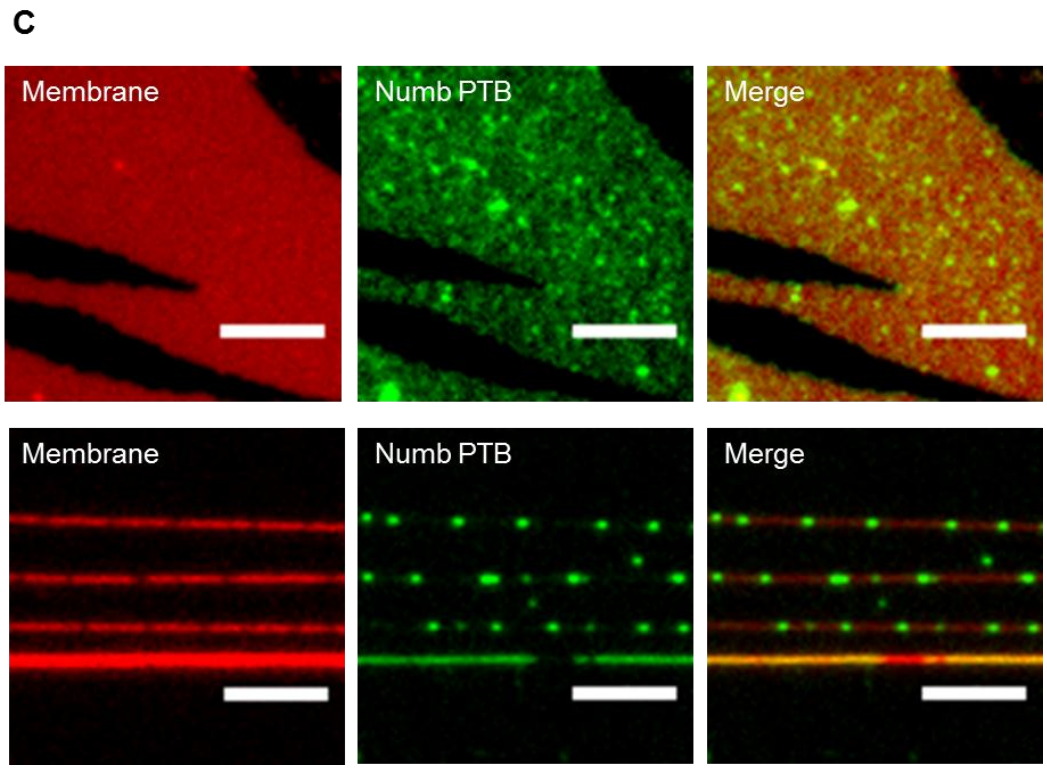

Figure 4.6 Oligomerization is the function of the Numb PTB (A) Comparison of effect of equally recruited Dab2 and Numb on membrane tubes highlighting membrane-active property of Numb (Top two panels). Numb PTB alone is able to constrict membrane tubes (third panel). Replacing PTB domain of Numb with Dab2 PTB impairs its ability to remodel membranes (bottom panel). (B) COV of membrane fluorescence of all constructs shown in A. (C) Al_{488} Maleimide-Numb PTB forms distinct cluster on SLB and tubes. All proteins (200nM) recruited by their N-terminal hexahistidine-tag.

Discussion

The peripheral membrane-bound protein Numb localizes to both the clathrin-coated structures at the plasma membrane [30] and perinuclear endosomes[20,33], although is precise role in regulating receptor traffic from these compartments is unclear. Target-membrane recognition by Numb is at-least in-part determined by specific binding to phospholipids[75] and cargo-receptors. Here, using these determinants, Numb was recruited to membrane using either PIP_2 or the cargo mimic $NPC1L1_{1266-1332}$. The mode of recruitment highlighted differences in organization of Numb. While on PIP_2 membranes Numb preferentially bound highly curved-tubes over planar bilayers, NPC1L1 recruited Numb independent of membrane-curvature. Remarkably, irrespective of the mode of recruitment, Numb organized as distinct clusters upon membrane binding. Numb clusters were membrane-active and produced constrictions on tubes that co-localized with the clusters. This is reminiscent of dynamin scaffolds that similarly constrict membrane tubes[72]. Recently a pull-down based

study has suggested Numb to be able to dimerize[21]. The membrane-active clusters of Numb could indeed reflect higher-order oligomers of the protein. Recently crowding by large unstructured regions on adaptors proteins has been proposed to facilitate membrane-bending [81,82]. Comparative analyses of artificially-recruited PTB-domain containing adaptors revealed that the ability to oligomerize is intrinsic and unique to Numb. Furthermore, the Numb PTB domain is sufficient to organize as clusters and constrict membrane tubes. Of note, between different organisms the PTB domain remains the most conserved part of Numb.

Oligomerization of Numb via its PTB domain may serve to cluster and sort receptors into a nascent vesicle. During division of the sensory organ precursor cell in *drosophila* Numb gets asymmetrically segregated by forming a tight crescent on the plasma membrane of one of the dividing cells. The mechanism of this segregation is not yet clear and indeed ability to self-oligomerize may be implicated in aiding the formation of the Numb crescent.

Reshaping of an initially flat membrane to highly curved bud is essential for vesicle formation. Several mechanisms of membrane remodeling have been proposed and specific endocytic proteins have been suggested to be involved in membrane reshaping [83]. Of the clathrin-adaptors, only epsin1 is a membrane-active protein that can sense curvature and tubulate liposomes via the PIP_2-binding ENTH domain and is essential for driving curvature and maturation of clathrin-coated vesicles [6,43]. The property to Numb to sense curvature in conjunction with its ability to remodel membranes may allow it to participate in later stages of vesicle budding where it may be involved in further deformation of the membrane.

Lately, the structural organization of endocytic adaptors is thought to be essential for linking clathrin polymerization to membrane bending. Disrupting the hetero-oligomeric interphase of yeast clathrin adaptors Sla2 and Ent1 has shown to impair vesicle maturation[84,85]. In this regards, it would be of great interest to locate the oligomerization interphase on the Numb PTB allowing analysis of the contribution of Numb-clustering to vesicle formation. Of relevance, there are two known of Numb that vary in their PTB domains (PTBo lacking or PTBi containing an 11-amino acid insert, 68–78 aa). The isoforms vary in their lipid binding, sub-cellular localization, as well as receptor recognition properties where only the shorter PTBo can bind NPC1L1[19,28,75]. It would be interesting to see if the membrane-active oligomerization abilities reported here are conserved between the PTB isoforms.

Chapter 5

Real-time visualization of Numb-mediated clathrin assembly

5.1 Introduction

Traditionally the contribution of interactions between membrane lipids and adaptor proteins to clathrin-polymerization has been understood by several minimal reconstitution-based assays [48,86]. Liposome sedimentation followed by EM imaging has provided information on lipid specificities and clathrin interacting abilities of various adaptor proteins[86]. Fluorescence microscopy based reconstitution studies on GUVs have studied the effect of membrane tension on adaptor protein mediated clathrin-assembly[48]. Reconstitution-assays on lipid-monolayer and unroofed cells with addition of purified components or cytosol paired with high-resolution EM have also been used to understand the contribution of individual endocytic proteins to membrane budding[87,88]. These approaches do not allow washing of excess unbound adaptor-proteins before introducing clathrin into the mixture, thereby raising the possibility of clathrin polymerizing into empty cages in solution. In addition, the entire process of building a canonical-CCV is completed in about 60 seconds[2]. The rate at which an adaptor assembles the clathrin-basket should therefore fall in this timescale. Available assays being based on end-point observations do not provide information on the kinetics of adaptor-mediated clathrin assembly.

SMrT has the advantage of following protein-protein interactions in real time allowing calculation of reaction kinetics[10,45]. Moreover, the flow-chamber that houses these templates allows control over washing of unbound proteins ensuring their interaction on the membrane. SMrTs are used here to follow Numb-mediated clathrin-assembly in real-time and over different membrane topologies.

5.2 Methods

5.2.1 Cloning, expression and protein purification

Clathrin heavy chain (Origene plasmid- SC125754) was cloned into pET15B with a C-terminal StrepII tag. For recombinant clathrin purification, clathrin heavy chain with a C-terminal StrepII tag was expressed in BL21(DE3) at 18 °C in autoinduction medium (Formedium, Norfolk, UK). Frozen bacterial pellets were lysed in 250mM Tris, pH 8.5, 1mM DTT supplemented with a PIC tablet (Roche). The lysate was spun (18,000 g) and the supernatant flowed on a Streptactin column (GE), washed and eluted in buffer containing 250mM Tris pH 8.5, 2.5mM desthiobiotin. The peak fractions were collected and fluorescently labeled with 10 fold molar excess of thiol-reactive Texas Red C2 maleimide

dye (Invitrogen) for 1 hr at RT. The labelling reaction was quenched with 1 mM DTT. To enrich for assembly-competent triskelia, purified labelled CHC was dialysed against 20mM MES pH 6.2 buffer supplemented with 2mM CaCl2 (18 hours). The solution was spun at 100,000g (1 hour, 4°C) and the pellet containing assembled clathrin was collected. Almost all of the free dye was seen in the supernatant. The pellet was resuspended in 10mM Tris pH 8.5 buffer supplemented with 0.5mM DTT by intermittent trituration (3 hr, RT). The solution was spun to remove any insoluble aggregates and the supernatent flash-frozen with 10% v/v glycerol. A typical prep yielded 1-2µM CHC that remained functional for about 3 months when stored at -80°C.

Native clathrin was extracted from clathrin-coated vesicles isolated from goat brains as described earlier[89] with a few modifications[45].

5.2.2 Fluorescent labelling of proteins

The purified CHC and native clathrin was labelled using 10 fold molar excess of thiol-reactive Texas Red C2 maleimide dye for 1 hr at RT. The reaction was quenched by addition of DTT. Free dye was removed in the subsequent dialysis steps. Labelled protein was judged to be free of unreacted dye by resolving on 10% SDS-PAGE.

5.2.3 Supported Membrane Templates (SMrT)

For clathrin-assembly reactions SMrTs were made with the lipid composition–DOPC: DOPS: DGSNTA(Ni^{2+}): DiD (79:15:5:1 mol%) as described in Methods section 4.2.3.

5.2.4 Fluorescence imaging

The fluorescence imaging was performed as described in Methods section 4.2.4.

5.2.5 Clathrin assembly reactions

SMrTs were made in filtered and degassed assay buffer HKS (20mM HEPES pH 7.4, 150mM KCl). To avoid non-specific sticking of clathrin, chamber was passivated with 1mg/ml of BSA. 200µl of 200nM adaptor-proteins were then incubated for 10 mins and washed with 3x200µl of HKS. To avoid any photo-toxicity and bleaching during continuous real-time imaging the chamber was equilibrated with oxygen-scavenger cocktail containing 0.2 mg/ml glucose oxidase (Sigma, G-2133), 0.035 mg/ml catalase (Sigma, C-40), 4.5 mg/ml

glucose, and 1mM DTT. Clathrin assembly reaction was monitored in real-time by flowing in 200µl of 100nM Texas Red-labeled clathrin or CHC, freshly diluted in HKS.

5.2.6 Image analysis

Fiji was used to analyze the fluorescence micrographs and time-lapse movies (Schindelin et al. 2012), and nonlinear regression analyses were carried out using GraphPad Prism as described previously. Kinetics of clathrin assembly were calculated as described previously[45]. Briefly, dead time of the flow cell was estimated in situ for each experiment by calculating the onset of fluorescent clathrin into the microscope field using a plateau followed by one-phase exponential rise function. Frames before the calculated onset were removed from time-lapse sequences. The background-corrected kymographs were generated from lines placed across the entire length of the membrane tube. Pixel intensity versus time data for all pixels on a kymograph were exported and fitted to a plateau followed by one-phase exponential rise function. Mean time constants were plotted from fits with an R^2 ≥0.8, which sorted out artifacts caused by microscope focus drifts and/or flow-induced lateral movement of foci.

5.3 Results

5.3.1 Real-time visualization of Numb-mediated clathrin-assembly

In order to visualize clathrin assembly, Numb (200nM) was first displayed on SMrTs containing chelating lipids. Artificially recruited Numb has the advantage of enabling comparison with clathrin-assembly properties of other CLASPs [10]. Upon incubation of Numb with SMrTs, characteristic constrictions developed on the membrane tubes owing to PTB mediated Numb clustering (Fig 5.1A Left-most panel, also see Fig 4.4). Excess, unbound Numb was washed thrice with 200 µl of HKS. The chamber was first equilibrated with oxygen scavenger cocktail (See Methods section 5.2.5) to reduce bleaching during stream acquisition. 100nM of fluorescently labelled native clathrin was then flowed in and imaged continuously at a high temporal resolution (100ms/frame). As clathrin entered the field of view, the background fluorescence intensity increased and distinct punctae of clathrin started forming on tubes. These punctae acted as nucleation-points and immediately grew brighter as they recruited more clathrin, indicative of co-operativity in clathrin-assembly. Within a minute, the build-up of clathrin fluorescence intensity on the punctae reached saturation (Fig 5.1 A). The clathrin foci were stable and showed little movement along the tube (see kymograph in Fig 5.1 B).

The kymographs reflecting build-up of clathrin fluorescence on a single tube were generated. The mean clathrin intensity along the length of the tube versus time data were extracted from kymographs, fitted to a plateau followed by a single exponential rise function and used to calculate τ, which reflects the assembly kinetics along the radius of the tube (see Methods 5.1.6) (Fig 5.1 C). The τ for Numb-mediated clathrin assembly was 53±12 sec, which falls in the range of the values reported for other CLASPs (Fig 5.1 D).

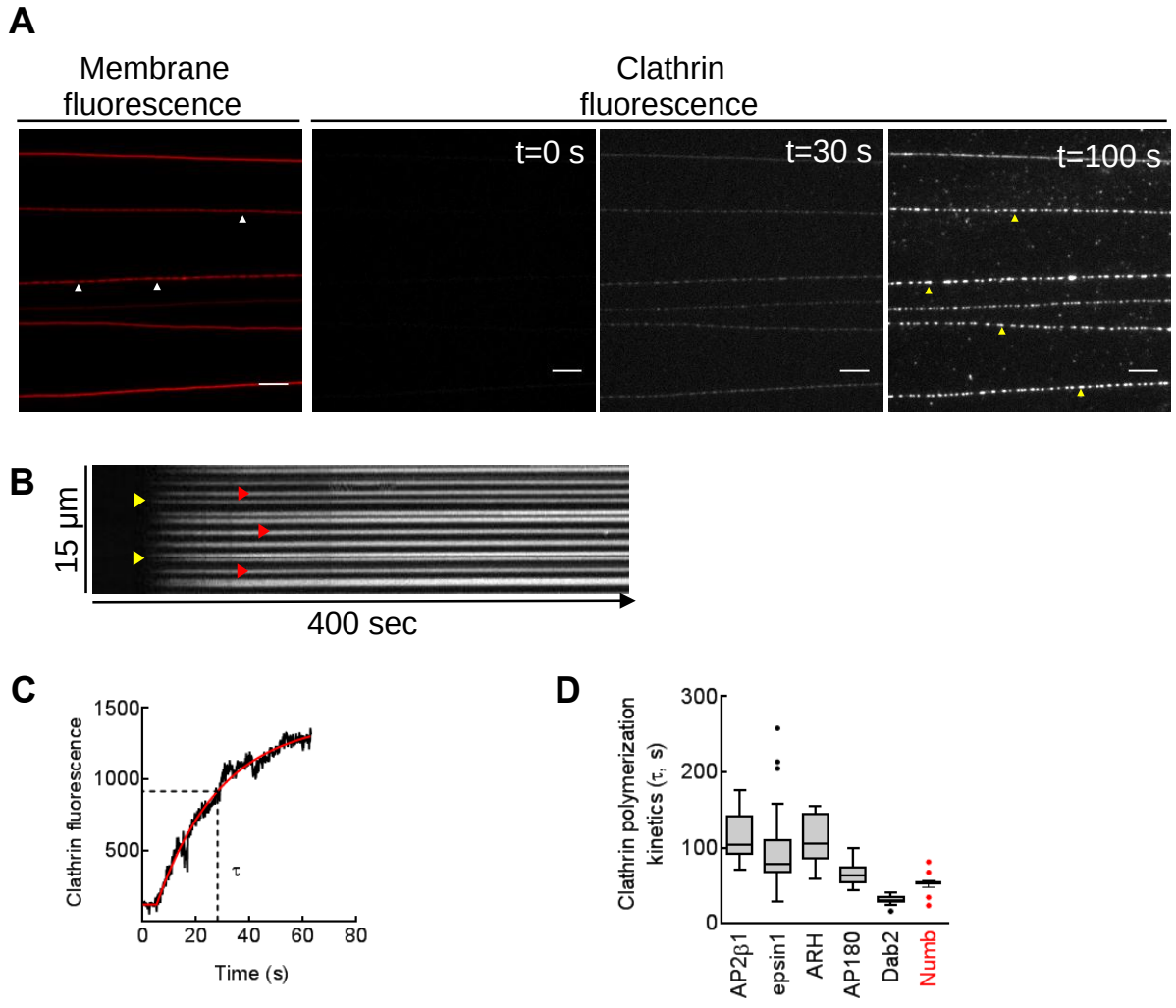

Figure 5.1 Kinetics of Numb-mediated clathrin-assembly (A) An array of tubes coated with Numb showing marked constrictions (white arrow-heads). Time lapse of tubes acquired after flowing in fluorescently-labelled clathrin. Yellow arrowheads point to the clathrin foci. (B) Representative kymograph from one Numb-coated tube showing clathrin-assembly. Yellow arrowheads point to the entry of clathrin and red arrows point to start of formation of clathrin puncate on tubes. (C) Trace of the build-up of clathrin fluorescence intensity along a single tube (black line) fitted to plateau-followed by one phase association kinetics (Red line). The dotted line indicates the t_{half} or τ. (D) t_{half} (τ) of clathrin assembly by Numb (53 sec) is comparable to that of the previously reported clathrin-adaptors (18 tubes from 3 independent experiments were analysed). The data-sets for previously-reported adaptors (in grey) are from [10].

5.3.2 Characteristics of clathrin-assembly by Numb

To co-relate Numb and clathrin distribution over varying membrane topologies, clathrin-assembly was carried out with Numb-mEGFP. For the sake of simplicity of protocol, clathrin heavy chain (CHC) used here was recombinantly expressed and purified (as described in Methods 5.2.1). Briefly, BL21(DE3) cells expressing CHC with a C-terminal StrepII tag were lysed in 250mM Tris pH 8.5 buffer supplemented 1mM DTT and 1mM EDTA (buffer was chosen to maintain clathrin as disassembled triskelia). CHC-StrepII was purified using affinity-chromatography and subsequently fluorescently labelled. To enrich for functional triskelia, CHC was assembled by dialysis against 20mM MES buffer supplemented with 2mM CaCl2 pH 6.2. The assembled cages were collected by a high-speed spin (Note- Significant amount of purified CHC was found in the pellet. Free, unreacted dye was separated in the supernatant). Clathrin lattices were disassembled in 10mM Tris pH 8.5 by trituration. To remove disassembly-resistant aggregates of CHC, the solution was again subjected to a high-speed spin (Fig 5.2A). The supernatant containing labelled, assembly-competent triskelia was diluted in HKS just before its use in the real-time clathrin assembly assays. Purified CHC was also tested using an antibody against the N-terminal domain of clathrin (Ab 24578). Recombinantly expressed CHC purified similarly was recently used to analyse the mechanism of Hsc70 mediated-clathrin cage disassembly[90].

Recombinant CHC was first tested by carrying out clathrin-assembly assays using the canonical clathrin-adaptor protein AP-2 β[47]. TxRed-CHC was flowed-in on SMrTs displaying AP-2β (recruited via chelating lipids) and imaged. As reported with native clathrin, CHC coated the tubes almost uniformly with very little clustering observed (Fig 5.2B). Of note, the rate of CHC-assembly appeared to be slower than that observed with native clathrin (data not shown). Control experiments where the adaptor was replaced with a 6xHis-tagged mEGFP showed no recruitment of CHC to the membrane (Fig 5.2C).

Next CHC-assembly was carried out with Numb-mEGFP. Foci of CHC assembled on tubes and were co-localized with Numb scaffolds over regions of tube constrictions (Fig 5.2D, E). Remarkably, although Numb was pre-arranged as scaffolds on both tubes and SLBs, CHC assembled in a curvature-dependent manner and was enriched on membrane tubes (Fig 5.2F).

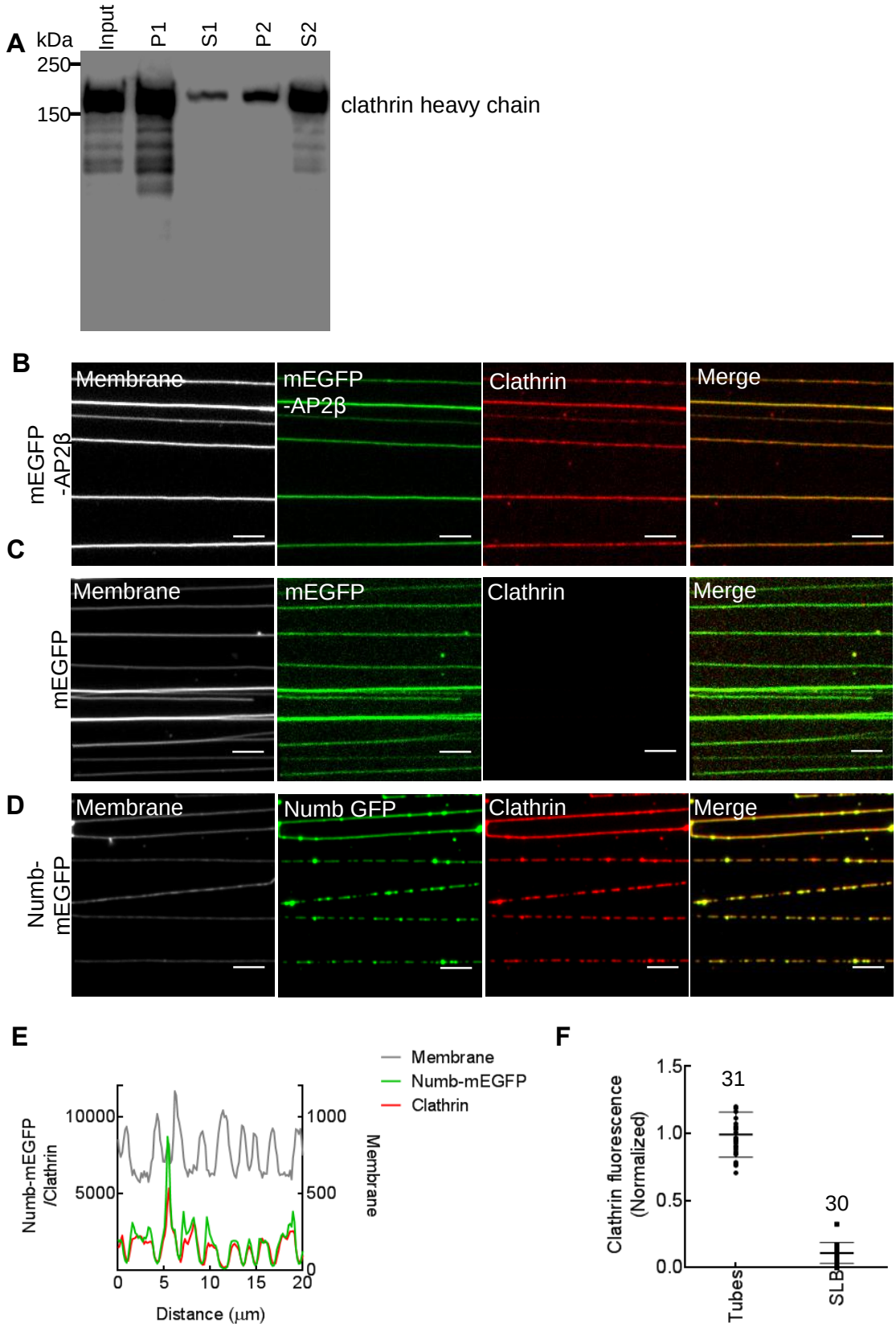

Figure 5.2 Characteristic of Numb-mediated clathrin-assembly (A) Commassie-stained 10% SDS-PAGE gel showing purification of assembly-competent CHC triskelia. Purified CHC (Input) on dialysis against the assembly buffer and subsequent spin was recovered in pellet (pellet-P1, supernatant-S1). Clathrin cages were

disassembled by trituration in disassembly buffer and subjected to high-speed spin. Most of CHC was recovered in the supernatant (Pellet-P2, supernatant-S2). (B) Fluorescent CHC (Red) was incubated with AP2-β (Green). CHC coated AP2-β-displaying tubes (Merge). (C) CHC (Red) does not bind tubes when the adaptor is replaced with mEGFP (Green). (D) CHC foci (Red) assembled on clusters of Numb-mEGFP (Green). (E) Numb-mEGFP clusters (Green line) assembled CHC (Red line) on regions on membrane constrictions (Grey line). (F) Numb-mEGFP assembles clathrin more efficiently on curved membrane tubes than on planar bilayers. Data represents mean ±SD of clathrin fluorescence normalized to Numb-mEGFP intensity.

5.4 Discussion

Real-time reconstitution of the Numb-clathrin interaction described here reveals the rate of clathrin-polymerization to be similar to that of the reported CLASPs emphasizing the ability of Numb to assemble clathrin in physiologically-relevant timescales. Numb could bind and assemble purified native clathrin further validating the interaction uncovered by SUPER template pull-down assays. The ability of Numb to self-oligomerize distinguishes it from the previously-tested CLASPs which cluster only in response to clathrin-assembly[10].

Furthermore, Numb-mEGFP scaffolds directed assembly of clathrin heavy chain (CHC) on regions of tube constriction. Although Numb was organised as clusters on both SLB and tubes, clathrin assembled in a curvature dependent manner and was enriched on the highly curved tubes.

Discussion

Numb, an evolutionarily conserved protein is essential for the clathrin-mediated transport of a class of receptors containing the FXNPXY sorting signal. Numb function was first discovered due to its involvement in *Drosophila* development. During asymmetrical division of the neural progenitor cell, Numb is segregated to the plasma membrane of one of the dividing cells. The asymmetry set in by Numb distribution confers alternate fates on the two progeny cells. The cell inheriting Numb divides to form neuron and sheath cells, while the other divides to become socket and hair cells. Collective work later established that Numb physically interacts and antagonizes Notch-receptor signalling in the Numb-enriched daughter cell activating specific pathways.

The segregation of Numb into a tight crescent at the basal-cortex of the dividing-progenitor cell is strikingly different from the gradient-like distribution of other patterning and requires the concerted action of several proteins. One of the critical factors is Miranda, the highly coiled-coil domain containing protein, which localizes to the plasma membrane and sequesters the transcription factor, Prospero. Polarity proteins Prospero, Miranda and PON (Partner of Numb) form crescent similar to Numb and are required for proper Numb distribution[91,92]. Par polarity complex and the associated kinase aPKC contribute to this process by excluding the polarity proteins [30]. Asymmetric distribution of mRNA is thought to drive the segregation of Prospero and Miranda but not Numb localization[93]. Interestingly quantitative live analysis of GFP- Pon and Numb-GFP fluorescence coupled with fluorescence recovery after photobleaching (FRAP) studies establish that both Numb and Pon rapidly exchange between the cytoplasmic pool and plasma membrane, and preferential recruitment from the cytoplasm is responsible for their asymmetric distribution during mitosis[94].

However, the molecular basis for how densely concentrated Numb crescents autonomously form in restricted membrane regions, the interactions that maintain these Numb assemblies, and the cues that trigger the clustering during mitosis are however still unclear. In this regard, a recent study reports a PON-Numb interaction that leads to a liquid-liquid phase-separation and formation of protein condensates in solution[95]. However, how the properties of the Numb-PON inter-protein interaction on membrane surfaces is still unclear. Using SMrT templates containing membranes of varying topologies, the results described in this thesis identify an intrinsic ability of Numb to self-oligomerize upon membrane-binding.

Surprisingly Numb oligomers on membrane tubes also lead to its constriction. Moreover, the property to self-oligomerize and remodel membranes was mapped to the PTB domain of Numb. Interestingly the PTB domain is shown to be essential to form condensed crescents during asymmetric cell-division[96]. In this context, it would be highly significant to identify the oligomerization interface on the Numb PTB and thereby test the contribution of the self-oligomerization ability of Numb to the formation of the condensed crescent during asymmetric cell division. The membrane-binding determinants tested here also show that PIP_2 alone is not sufficient for recruitment of Numb to planar SLB. However artificial recruitment with chelating lipids or presence of receptor aids binding as well as clustering. These results suggest the involvement of a membrane-protein to facilitate recruitment of Numb during crescent formation. Upon initial membrane localization, the intrinsic PTB-mediated oligomerization ability could act to enable clustering of Numb.

Numb is thought to antagonize Notch signaling by decreasing Notch levels on the plasma membrane. The many models proposed suggest that Numb reduces Notch on the plasma membrane by- promoting endocytosis, inhibiting recycling from the endosomes, and promoting degradation of Notch. Numb function in development reiterates its involvement in regulating receptor distribution by participating in clathrin-mediates vesicular transport. Numb is proposed to regulate receptor distribution by participating in either receptor internalization from the plasma membrane as well as recycling and degradation of endocytosed receptors from the early endosomes. However, what regulates Numb recruitment to different target organelles and the mechanism of how it links the cargo-receptors to the clathrin-transport machinery is still lacking.

In an effort to investigate Numb functions, a novel pull-down approach with adaptors displayed on lipid bilayer coated silica beads (SUPER templates) was standardized. Using membrane-displayed Numb as the bait, this work reports for the first time a direct interaction between Numb and clathrin was uncovered. The clathrin-binding attributes on Numb were determined using a series of deletions spanning the entire sequence of Numb that were tested for CHC-binding. Using a combination of a facile dot-blot assay and SUPER template-based pull-downs, the PRR (proline-rich region) was identified as the clathrin interacting region on Numb. Furthermore, transient expression of Numb PRR inhibited transferrin-uptake in Cos7 cells. SUPER pull-downs also show that the Numb-clathrin interaction is supressed by AP2-binding.

Although the functional significance of this interactions is not clear yet, it may contribute to Numb's role is regulating receptor trafficking from the endosomes. While clear experimental

evidence indicates that Numb induces endocytosis of NPC1L1, integrin and EAAT3 in a clathrin and AP-2-dependent manner depositing these at the early endosomes, the contribution of Numb to the regulation of Notch distribution is still unclear. Interestingly, imaging of fluorescently-tagged Numb in *Drosophila* revealed that Numb is dispensable for internalization of Notch but functions by co-accumulating with Notch (and Spdo) in sub-apical endosomes and inhibiting Notch recycling back to the plasma membrane[32]. Cellular studies tracking localisation of surface-labelled Notch indicates Numb promotes post-endocytic degradation of Notch[33,34]. Similar to Notch, Increasing experimental evidence now points to the involvement of Numb in regulating transport from the early endosomes[34,36,97]. Early endosomes sort cargo either into the degradative pathway to lysosomes or into the recycling route to the plasma membrane[16,98]. One major difference between the clathrin-coated carriers made at the early endosomes and the plasma membrane is the sorting of cargo for transport to different routes that must occur when the carrier is built at the early endosomes. Both the fast and slow recycling pathways from the early endosomes recruit clathrin via Rab4a/b dependent mechanisms and require AP-1 and GGA3 [65,66]. However, given the co-ordination of vesicle formation events that sorting of cargo at the early endosomes must necessitate, the full repertoire of protein machinery and the clathrin-adaptors needed to make these recycling vesicles and tubules is likely to be far more complex. Numb with its intrinsic ability to self-assemble into separate clusters, and polymerize clathrin could indeed serve as a potential endosomal clathrin-adaptor.

Collectively this works identifies two biochemical properties of Numb- the PTB domain binds membrane consequently leading to self-oligomerization to form clusters while the PRR independently recruits clathrin. Although the PRR is sufficient to bind clathrin in SUPER pull-down assays, whether the kinetics of clathrin-polymerization are similar to full-length Numb is not yet clear. Real-time visualization of clathrin assembly with PRR and Numb can be compared to analyse the contribution of PTB-aided clustering to PRR-mediated clathrin polymerization. Moreover, both the PTB and PRR are alternatively spliced in cells and the resulting isoforms are proposed to exert different function causing alternate developmental fates[27,29]. Recently, Numb isoform that vary in the PRR (p66 and p72) were seen to regulate the balance between receptor recycling and degradation from the early endosomes, presumably by recruiting different partners[69]. Whether the properties identified here are similar between Numb-isoforms remains to be tested.

References

1. Taylor, M. J., Perrais, D. & Merrifield, C. J. A high precision survey of the molecular dynamics of mammalian clathrin-mediated endocytosis. *PLoS Biol.* **9**, (2011).

2. Ehrlich, M. *et al.* Endocytosis by random initiation and stabilization of clathrin-coated pits. *Cell* **118**, 591–605 (2004).

3. Kaksonen, M. & Roux, A. Mechanisms of clathrin-mediated endocytosis. *Nat. Rev. Mol. Cell Biol.* **19**, 313–326 (2018).

4. Wilhelm, B. G. *et al.* Composition of isolated synaptic boutons reveals the amounts of vesicle trafficking proteins. *Science (80-.).* **344**, 1023–1028 (2014).

5. Schmid, E. M. *et al.* Role of the AP2 beta-appendage hub in recruiting partners for clathrin-coated vesicle assembly. *PLoS Biol.* **4**, 1532–1548 (2006).

6. Ford, M. G. J. Simultaneous Binding of PtdIns(4,5)P2 and Clathrin by AP180 in the Nucleation of Clathrin Lattices on Membranes. *Science (80-.).* **291**, 1051–1055 (2001).

7. Engqvist-Goldstein, Å. E. Y. *et al.* The actin-binding protein Hip1R associates with clathrin during early stages of endocytosis and promotes clathrin assembly in vitro. *J. Cell Biol.* **154**, 1209–1223 (2001).

8. Mishra, S. K. *et al.* Disabled-2 exhibits the properties of a cargo-selective endocytic clathrin adaptor. *EMBO J.* **21**, 4915–4926 (2002).

9. He, G. *et al.* ARH is a modular adaptor protein that interacts with the LDL receptor, clathrin, and AP-2. *J. Biol. Chem.* **277**, 44044–44049 (2002).

10. Pucadyil, T. J. & Holkar, S. S. Comparative analysis of adaptor-mediated clathrin assembly reveals general principles for adaptor clustering. *Mol. Biol. Cell* **27**, 3156–3163 (2016).

11. Motley, A., Bright, N. A., Seaman, M. N. J. & Robinson, M. S. Clathrin-mediated endocytosis in AP-2-depleted cells. *J. Cell Biol.* **162**, 909–918 (2003).

12. Robinson, M. S. Adaptable adaptors for coated vesicles. *Trends Cell Biol.* **14**, 167–174 (2004).

13. Reider, A. & Wendland, B. Endocytic adaptors - social networking at the plasma membrane. *J. Cell Sci.* **124**, 1613–1622 (2011).

14. Keyel, P. A., Watkins, S. C. & Traub, L. M. Endocytic Adaptor Molecules Reveal an Endosomal Population of Clathrin by Total Internal Reflection Fluorescence Microscopy. *J. Biol. Chem.* **279**, 13190–13204 (2004).

15. Scott, P. M. *et al.* GGA proteins bind ubiquitin to facilitate sorting at the trans-Golgi network. *Nat. Cell Biol.* **6**, 252–259 (2004).

16. Hsu, V. W. & Prekeris, R. Transport at the recycling endosome. *Curr. Opin. Cell Biol.* **22**, 528–534 (2010).

17. Bonifacino, J. S. & Rojas, R. Retrograde transport from endosomes to the trans-Golgi network. *Nat. Rev. Mol. Cell Biol.* **7**, 568–579 (2006).

18. Nishimura, T. & Kaibuchi, K. Numb Controls Integrin Endocytosis for Directional Cell Migration with aPKC and PAR-3. *Dev. Cell* **13**, 15–28 (2007).

19. Li, P. S. *et al.* The clathrin adaptor Numb regulates intestinal cholesterol absorption through dynamic interaction with NPC1L1. *Nat. Med.* **20**, 80–86 (2014).

20. Santolini, E. *et al.* Numb is an endocytic protein. *J. Cell Biol.* **151**, 1345–1351 (2000).

21. Hirai, M. *et al.* Adaptor proteins NUMB and NUMBL promote cell cycle withdrawal by targeting ERBB2 for degradation. *J. Clin. Invest.* **127**, 569–582 (2017).

22. Kyriazis, G. A. *et al.* Numb endocytic adapter proteins regulate the transport and processing of the amyloid precursor protein in an isoform-dependent manner: Implications for Alzheimer disease pathogenesis. *J. Biol. Chem.* **283**, 25492–25502 (2008).

23. Su, J.-F. *et al.* Numb directs the subcellular localization of excitatory amino acid transporter type 3 through binding the YXNXXF motif. *J. Cell Sci.* jcs.185496 (2016). doi:10.1242/jcs.185496

24. Sato, K. *et al.* Numb controls E-cadherin endocytosis through p120 catenin with

aPKC. *Mol. Biol. Cell* **22**, 3103–3119 (2011).

25. Rhyu, M. S., Jan, L. Y. & Jan, Y. N. Asymmetric distribution of numb protein during division of the sensory organ precursor cell confers distinct fates to daughter cells. *Cell* **76**, 477–491 (1994).

26. Frise, E., Knoblich, J. A., Younger-Shepherd, S., Jan, L. Y. & Jan, Y. N. The Drosophila Numb protein inhibits signaling of the Notch receptor during cell-cell interaction in sensory organ lineage. *Proc. Natl. Acad. Sci.* **93**, 11925–11932 (1996).

27. Wei, J. *et al.* The clathrin adaptor proteins ARH, Dab2, and numb play distinct roles in Niemann-Pick C1-Like 1 versus low density lipoprotein receptor-mediated cholesterol uptake. *J. Biol. Chem.* **289**, 33689–33700 (2014).

28. Dho, S. E., French, M. B., Woods, S. A. & McGlade, C. J. Characterization of Four Mammalian Numb Protein Isoforms. *J. Biol. Chem.* **274**, 33097–33104 (1999).

29. Verdi, J. M. *et al.* Distinct human NUMB isoforms regulate differentiation vs. proliferation in the neuronal lineage. *Neurobiology* **96**, 10472–10476 (1999).

30. Smith, C. A. *et al.* aPKC-mediated phosphorylation regulates asymmetric membrane localization of the cell fate determinant Numb. *EMBO J.* **26**, 468–480 (2007).

31. Krieger, J. R. *et al.* Identification and Selected Reaction Monitoring (SRM) Quantification of Endocytosis Factors Associated with Numb. *Mol. Cell. Proteomics* **12**, 499–514 (2013).

32. Couturier, L., Mazouni, K. & Schweisguth, F. Numb localizes at endosomes and controls the endosomal sorting of notch after asymmetric division in drosophila. *Curr. Biol.* **23**, 588–593 (2013).

33. McGill, M. A., Dho, S. E., Weinmaster, G. & McGlade, C. J. Numb regulates post-endocytic trafficking and degradation of notch1. *J. Biol. Chem.* **284**, 26427–26438 (2009).

34. Johnson, S. A., Zitserman, D. & Roegiers, F. Numb regulates the balance between Notch recycling and late-endosome targeting in Drosophila neural progenitor cells. *Mol. Biol. Cell* **27**, 2857–2866 (2016).

35. Tang, H. *et al.* Numb Proteins Specify Asymmetric Cell Fates via an Endocytosis- and Proteasome-Independent Pathway. *Mol. Cell. Biol.* **25**, 2899–2909 (2005).

36. Nilsson, L., Jonsson, E. & Tuck, S. Caenorhabditis elegans Numb Inhibits Endocytic Recycling by Binding TAT-1 Aminophospholipid Translocase. *Traffic* **12**, 1839–1849 (2011).

37. Kirchhausen, T. THREE WAYS TO MAKE A VESICLE. *Nat. Rev. Mol. Cell Biol.* **1**, 187–198 (2000).

38. Bigay, J., Casella, J. F., Drin, G., Mesmin, B. & Antonny, B. ArfGAP1 responds to membrane curvature through the folding of a lipid packing sensor motif. *EMBO J.* **24**, 2244–2253 (2005).

39. Christis, C. & Munro, S. The small G protein Arl1 directs the trans-Golgi-specific targeting of the Arf1 exchange factors BIG1 and BIG2. *J. Cell Biol.* **196**, 327–335 (2012).

40. Bubeck, P., Winkler, M. & Bautsch, W. Rapid cloning by homologous recombination in vivo. *Nucleic Acids Res.* **21**, 3601–2 (1993).

41. Pucadyil, T. J. & Schmid, S. L. Supported bilayers with excess membrane reservoir: A template for reconstituting membrane budding and fission. *Biophys. J.* **99**, 517–525 (2010).

42. Pucadyil, T. J. & Schmid, S. L. Real-time visualization of dynamin-catalyzed membrane fission and vesicle release. *Cell* **135**, 1263–75 (2008).

43. Messa, M. *et al.* Epsin deficiency impairs endocytosis by stalling the actin-dependent invagination of endocytic clathrin-coated pits. *Elife* **3**, 1–25 (2014).

44. Drake, M. T., Downs, M. a. & Traub, L. M. Epsin Binds to Clathrin by Associating Directly with the Clathrin-terminal Domain. *J. Biol. Chem.* **275**, 6479–6489 (2000).

45. Holkar, S. S., Kamerkar, S. C. & Pucadyil, T. J. Spatial control of epsin-induced clathrin assembly by membrane curvature. *J. Biol. Chem.* **290**, 14267–14276 (2015).

46. Rosenthal, J. A. *et al.* The epsins define a family of proteins that interact with components of the clathrin coat and contain a new protein module. *J. Biol. Chem.* **274**,

33959–33965 (1999).

47. Kelly, B. *et al.* AP2 controls clathrin polymerization with a membrane-activated switch Bernard. *Science (80-.).* **345**, 459–463 (2014).

48. Saleem, M. *et al.* A balance between membrane elasticity and polymerization energy sets the shape of spherical clathrin coats. *Nat. Commun.* **6**, (2015).

49. Mishra, S. K. *et al.* Dual engagement regulation of protein interactions with the AP-2 adaptor α appendage. *J. Biol. Chem.* **279**, 46191–46203 (2004).

50. Praefcke, G. J. K. *et al.* Evolving nature of the AP2 α-appendage hub during clathrin-coated vesicle endocytosis. *EMBO J.* **23**, 4371–4383 (2004).

51. Lafer, E. M. Clathrin–Protein Interactions. *Traffic* **3**, 513–520 (2002).

52. Chen, X. *et al.* Structural determinants controlling 14-3-3 recruitment to the endocytic adaptor Numb and dissociation of the Numb α-adaptin complex. *J. Biol. Chem.* **293**, 4149–4158 (2018).

53. Sorensen, E. B. & Conner, S. D. AAK1 regulates Numb function at an early step in clathrin-mediated endocytosis. *Traffic* **9**, 1791–1800 (2008).

54. Ramjaun, A. R. & McPherson, P. S. Multiple amphiphysin II splice variants display differential clathrin binding: identification of two distinct clathrin-binding sites. *J. Neurochem.* **70**, 2369–76 (1998).

55. Dell'Angelica, E. C. Clathrin-binding proteins: Got a motif? Join the network! *Trends Cell Biol.* **11**, 315–318 (2001).

56. Mao, Y., Chen, J., Maynard, J. A., Zhang, B. & Quiocho, F. A. A novel all helix fold of the AP180 amino-terminal domain for phosphoinositide binding and clathrin assembly in synaptic vesicle endocytosis. *Cell* **104**, 433–440 (2001).

57. Haffner, C., Di Paolo, G., Rosenthal, J. A. & De Camilli, P. Direct interaction of the 170 kDa isoform of synaptojanin 1 with clathrin and with the clathrin adaptor AP-2. *Curr. Biol.* **10**, 471–474 (2000).

58. Edelstein, A., Amodaj, N., Hoover, K., Vale, R. & Stuurman, N. Computer control of microscopes using μManager. *Curr. Protoc. Mol. Biol.* 1–17 (2010).

doi:10.1002/0471142727.mb1420s92

59. Edelstein, A. D. *et al.* Advanced methods of microscope control using μManager software. *J. Biol. Methods* **1**, 10 (2014).

60. Maurer, M. E. & Cooper, J. A. The adaptor protein Dab2 sorts LDL receptors into coated pits independently of AP-2 and ARH. *J. Cell Sci.* **119**, 4235–4246 (2006).

61. Chan, L. S., Moshkanbaryans, L., Xue, J. & Graham, M. E. The, 16 kDa C-terminal sequence of clathrin assembly protein AP180 is essential for efficient clathrin binding. *PLoS One* **9**, (2014).

62. Moshkanbaryans, L., Xue, J., Wark, J. R., Robinson, P. J. & Graham, M. E. A novel sequence in AP180 and CALM promotes efficient clathrin binding and assembly. *PLoS One* **11**, 1–18 (2016).

63. Yap, C. C. & Winckler, B. Adapting for endocytosis: roles for endocytic sorting adaptors in directing neural development. *Front. Cell. Neurosci.* **9**, 1–17 (2015).

64. Zhao, X. *et al.* Expression of auxilin or AP180 inhibits endocytosis by mislocalizing clathrin: evidence for formation of nascent pits containing AP1 or AP2 but not clathrin. *J. Cell Sci.* **114**, 353–65 (2001).

65. Laura, P. *et al.* Rab4b controls an early endosome sorting event by interacting with the γ subunit of the clathrin adaptor complex 1. *J. Cell Sci.* (2013).

66. D'Souza, R. S. *et al.* Rab4 orchestrates a small GTPase cascade for recruitment of adaptor proteins to early endosomes. *Curr. Biol.* **24**, 1187–1198 (2014).

67. Poteryaev, D., Datta, S., Ackema, K., Zerial, M. & Spang, A. Identification of the switch in early-to-late endosome transition. *Cell* **141**, 497–508 (2010).

68. Girard, E. *et al.* Rab7 is functionally required for selective cargo sorting at the early endosome. *Traffic* **15**, 309–326 (2014).

69. Dagnino, L. *et al.* NUMB regulates the endocytosis and activity of the anaplastic lymphoma kinase in an isoform-specific manner. *J. Mol. Cell Biol.* (2019). doi:10.1093/jmcb/mjz003

70. McMahon, H. T. & Boucrot, E. Molecular mechanism and physiological functions of

clathrin-mediated endocytosis. *Nat. Rev. Mol. Cell Biol.* **12**, 517–33 (2011).

71. Várnai, P. *et al.* Inositol lipid binding and membrane localization of isolated pleckstrin homology (PH) domains. Studies on the PH domains of phospholipase C δ1 and p130. *J. Biol. Chem.* **277**, 27412–27422 (2002).

72. Dar, S., Kamerkar, S. C. & Pucadyil, T. J. A high-throughput platform for real-time analysis of membrane fission reactions reveals dynamin function. *Nat. Cell Biol.* **17**, 1588–1596 (2015).

73. Jung, H., Robison, A. D. & Cremer, P. S. Detecting protein-ligand binding on supported bilayers by local pH modulation. *J. Am. Chem. Soc.* **131**, 1006–1014 (2009).

74. Schindelin, J. *et al.* Fiji: an open-source platform for biological-image analysis. *Nat. Methods* **9**, 676–682 (2012).

75. Bailey, M. J. & Prehoda, K. E. Establishment of Par-Polarized Cortical Domains via Phosphoregulated Membrane Motifs. *Dev. Cell* **35**, 199–210 (2015).

76. Dar, S., Kamerkar, S. C. & Pucadyil, T. J. Use of the supported membrane tube assay system for real-time analysis of membrane fission reactions. *Nat. Protoc.* **12**, 390–400 (2017).

77. Kunding, A. H., Mortensen, M. W., Christensen, S. M. & Stamou, D. A fluorescence-based technique to construct size distributions from single-object measurements: Application to the extrusion of lipid vesicles. *Biophys. J.* **95**, 1176–1188 (2008).

78. Traub, L. M. Common principles in clathrin-mediated sorting at the Golgi and the plasma membrane. *Biochim. Biophys. Acta - Mol. Cell Res.* **1744**, 415–437 (2005).

79. Heldwein, E. E. *et al.* Crystal structure of the clathrin adaptor protein 1 core. *Proc. Natl. Acad. Sci.* **101**, 14108–14113 (2004).

80. Garcia, P. *et al.* The Pleckstrin Homology Domain of Phospholipase C-δ1 Binds with High Affinity to Phosphatidylinositol 4,5-Bisphosphate in Bilayer Membranes. *Biochemistry* **34**, 16228–16234 (1995).

81. Busch, D. J. *et al.* Intrinsically disordered proteins drive membrane curvature. *Nat. Commun.* **6**, 1–11 (2015).

82. Zeno, W. F. *et al.* Synergy between intrinsically disordered domains and structured proteins amplifies membrane curvature sensing. *Nat. Commun.* **9**, (2018).

83. Kozlov, M. M. *et al.* Mechanisms shaping cell membranes. *Curr. Opin. Cell Biol.* **29**, 53–60 (2014).

84. Garcia-Alai, M. M. *et al.* Epsin and Sla2 form assemblies through phospholipid interfaces. *Nat. Commun.* **9**, 1–13 (2018).

85. Skruzny, M. *et al.* An Organized Co-assembly of Clathrin Adaptors Is Essential for Endocytosis. *Dev. Cell* **33**, 150–162 (2015).

86. Dannhauser, P. N. & Ungewickell, E. J. Reconstitution of clathrin-coated bud and vesicle formation with minimal components. *Nat. Cell Biol.* **14**, 634–639 (2012).

87. Henne, W. M. *et al.* FCHo proteins are nucleators of Clathrin-Mediated endocytosis. *Science (80-.).* **328**, 1281–1284 (2010).

88. Lindsay, M. *et al.* Cell compartmentalisation in planctomycetes: novel types of structural organisation for the bacterial cell. *Arch. Microbiol.* **175**, 413–429 (2001).

89. Campbell, C., Squicciarini, J., Shia, M., Pilch, P. F. & Fine, R. E. Identification of a Protein Kinase as an Intrinsic Component of Rat Liver Coated Vesicles? *Am. Chem. Soc.* **23**, 31–38 (1984).

90. Sousa, R. *et al.* Clathrin-coat disassembly illuminates the mechanisms of Hsp70 force generation. *Nat. Struct. Mol. Biol.* **23**, 821–829 (2016).

91. Shen, C. P., Jan, L. Y. & Jan, Y. N. Miranda is required for the asymmetric localization of prospero during mitosis in Drosophila. *Cell* **90**, 449–458 (1997).

92. Lu, B., Ackerman, L., Jan, L. Y., Jan, Y. & Francisco, S. Modes of Protein Movement that Lead to the Asymmetric .pdf. *Mol. Cell* **4**, 883–891 (1999).

93. Schuldt, A. J. *et al.* Miranda mediates asymmetric protein and RNA localization in the developing nervous system. *Genes Dev.* **12**, 1847–1857 (1998).

94. Mayer, B., Emery, G., Berdnik, D., Wirtz-Peitz, F. & Knoblich, J. A. Quantitative analysis of protein dynamics during asymmetric cell division. *Curr. Biol.* **15**, 1847–1854 (2005).

95. Shan, Z. *et al.* Basal condensation of Numb and Pon complex via phase transition during Drosophila neuroblast asymmetric division. *Nat. Commun.* **9**, (2018).

96. Knoblich, J. A., Jan, L. Y. & Jan, Y. N. The N terminus of the Drosophila Numb protein directs membrane association and actin-dependent asymmetric localization. *Proc. Natl. Acad. Sci.* **94**, 13005–13010 (2002).

97. Cotton, M., Benhra, N. & Le Borgne, R. Numb inhibits the recycling of sanpodo in drosophila sensory organ precursor. *Curr. Biol.* **23**, 581–587 (2013).

98. Vanlandingham, P. A. & Ceresa, B. P. Rab7 regulates late endocytic trafficking downstream of multivesicular body biogenesis and cargo sequestration. *J. Biol. Chem.* **284**, 12110–12124 (2009).